Finite Volume and Finite Element Methods in CFD (Numerical Simulation of Compressible Flow)

M. Feistauer
Charles University Prague, Faculty of Mathematics and Physics

Charles University • Prague
2007

PREFACE

This text should serve as a source for the course delivered in April 2007 at the University of Vienna. The purpose of this course is to give a survey of recent methods and techniques for the numerical solution of compressible flow. The course follows the book

M. Feistauer, J. Felcman, I. Straškraba: *Mathematical and Computational Methods for Compressible Flow*, Clarendon Press, Oxford, 2004, ISBN 0 19 850588 4

where all details and a number of examples can be found.

The author gratefully acknowledges the invitation of Professor Christian Schmeiser to visit Univeristy of Vienna, allowing him to deliver this course.

Vienna, April 2007

Miloslav Feistauer
Charles University Prague
Faculty of Mathematics and Physics
Sokolovská 83, 186 75 Praha 8
Czech Republic
feist@karlin.mff.cuni.cz

CONTENTS

INTRODUCTION

Fluid dynamics is an amazing field which is important in many areas: machinery, aviations, aeronautics, car industry, chemistry, food industry, hydrology, meteorology, environmental protection, medicine,. . . .

An image of flow can be obtained in two ways:
a) With the aid of *experiments* (for example in wind tunnels). They are however expensive, lengthy and sometimes impossible. Let us mention flow around space vehicles at re-entry, loss-of-coolant accident in a nuclear reactor, medicine.
b) With the aid of mathematical models. Mathematical and numerical modelling allows to get qualitative as well as quantitative properties of flow. Under the qualitative properties we understand existence, uniqueness, stability, asymptotic behaviour etc. of the solution. The quantitative properties are obtained with the aid of numerical and computational methods applied on modern computers. The development of numerical simulation of fluid dynamical problems caused that (round 1950) Computational Fluid Dynamics (CFD) was constituted.

CFD is the area which is concerned with applications of mathematical, numerical and computational techniques to the fluid flow simulation.

The *main goal* of CFD is to obtain results comparable with wind tunnel experiments, to avoid (at least partially) expensive and time consuming measurements and to simulate process which cannot be realized experimentally.

CFD has several *ingredients*:

- mathematical models = starting point,
- rigorous mathematical analysis of numerical methods,
- heuristic approaches = heuristic extension of theoretical results to cases, where the pure mathematical analysis is not yet available,
- experience, comparison of computational results with experiments and then feedback leading to improvement of mathematical models and numerical methods.

One can say that CFD (similarly as numerical mathematics) has two faces: it is a rigorous mathematical science on one side, and an art on the other side.

In this course, we shall be concerned with one of the most difficult parts of CFD: *numerical simulation of compressible flow*. Here it is necessary to overcome several important *obstacles*:

- mixed hyperbolic-parabolic character of governing equations,
- nonlinearity of equations,
- simulation of convection dominating over diffusion,
- simulation of shock waves, boundary layers and wakes and their interaction,
- the lack of theoretical analysis for the continuous problem.

1

BASIC EQUATIONS

In this course we shall be concerned with the motion of compressible fluids, i.e. gases.

1.1 Governing equations and relations of gas dynamics

Let $(0,T) \subset I\!R$ be a time interval, during which we follow the fluid motion, and let $\Omega \subset I\!R^N,\ N = 1,2,3$, denote the domain occupied by the fluid. (For simplicity we assume that it is independent of t).

1.1.1 *Description of the flow*

There are two possibilities for describing the fluid motion: Lagrangean and Eulerian.

We shall use here the *Eulerian description* based on the determination of the *velocity* $\boldsymbol{v}(x,t) = (v_1(x,t), \dots,\ v_N(x,t))$ of the fluid particle passing through the point x at time t. We shall also use the state variables: p - pressure, ρ - density and θ - absolute temperature.

In what follows, we shall introduce the mathematical formulation of fundamental physical laws: the law of conservation of mass, the law of conservation of momentum and the law of conservation of energy, called in brief *conservation laws.*

1.1.2 *The continuity equation*

$$\frac{\partial \rho}{\partial t}(x,t) + \operatorname{div}(\rho(x,t)\boldsymbol{v}(x,t)) = 0, \qquad t \in (0,T),\ x \in \Omega \tag{1.1.1}$$

is the differential form of the law of conservation of mass.

1.1.3 *The equations of motion*

Basic dynamical equations describing fluid motion are derived from the *law of conservation of momentum.*

The equations of motion of general fluids

$$\frac{\partial}{\partial t}(\rho v_i) + \operatorname{div}(\rho v_i \boldsymbol{v}) = \rho f_i + \sum_{j=1}^{N} \frac{\partial \tau_{ji}}{\partial x_j}, \qquad i = 1, \dots, N. \tag{1.1.2}$$

This can be written as

$$\frac{\partial}{\partial t}(\rho \boldsymbol{v}) + \operatorname{div}(\rho \boldsymbol{v} \otimes \boldsymbol{v}) = \rho \boldsymbol{f} + \operatorname{div}\mathcal{T}. \tag{1.1.3}$$

Here $\boldsymbol{v}\otimes\boldsymbol{v}$ is the tensor with components $v_iv_j, i,j=1,\dots,N$, τ_{ij} are components of the stress tensor $\mathcal{T}$ and f_i are components of the outer volume force $\boldsymbol{f}$.

1.1.4 *The law of conservation of the moment of momentum; symmetry of the stress tensor*

Theorem 1.1 *The law of conservation of the moment of momentum is valid if and only if the stress tensor $\mathcal{T}$ is symmetric.*

1.1.5 *The Navier–Stokes equations*

The relations between the stress tensor and other quantities describing fluid flow, particularly the velocity and its derivatives, represent the so-called *rheological equations* of the fluid. The simplest rheological equation

$$\mathcal{T} = -p\,\mathbb{I}, \tag{1.1.4}$$

characterizes inviscid fluid. Here p is the pressure and $\mathbb{I}$ is the unit tensor:

$$\mathbb{I} = \begin{pmatrix} 1,\,0,\,0 \\ 0,\,1,\,0 \\ 0,\,0,\,1 \end{pmatrix} \quad \text{for } N=3. \tag{1.1.5}$$

Besides the pressure forces, the friction shear forces also act in real fluids as a consequence of the *viscosity*. Therefore, in the case of viscous fluid, we add a contribution $\mathcal{T}'$ characterizing the shear stress to the term $-p\,\mathbb{I}$:

$$\mathcal{T} = -p\,\mathbb{I} + \mathcal{T}'. \tag{1.1.6}$$

In order to identify the viscous part $\mathcal{T}'$ of the stress tensor, we shall use *Stokes' postulates* Then it is possible to show that the following representation holds true ((Feistauer, 1993)):

Theorem 1.2 *The stress tensor has the form*

$$\mathcal{T} = (-p + \lambda \operatorname{div}\boldsymbol{v})\,\mathbb{I} + 2\mu\mathbb{D}(\boldsymbol{v}), \tag{1.1.7}$$

where λ, μ are constants or scalar functions of thermodynamical quantities.

If the stress tensor depends linearly on the velocity deformation tensor as in (1.1.7), the fluid is called *Newtonian*, which is the case of gases.

We get the so-called *Navier–Stokes equations*

$$\begin{aligned} &\frac{\partial(\rho\boldsymbol{v})}{\partial t} + \operatorname{div}(\rho\boldsymbol{v}\otimes\boldsymbol{v}) \\ &= \rho\boldsymbol{f} - \operatorname{grad} p + \operatorname{grad}(\lambda \operatorname{div}\boldsymbol{v}) + \operatorname{div}(2\mu\mathbb{D}(\boldsymbol{v})). \end{aligned} \tag{1.1.8}$$

1.1.6 *Properties of the viscosity coefficients*

Here μ and λ are called the first and the second *viscosity coefficients*, respectively, μ is also called *dynamical viscosity*. In the kinetic theory of gases the conditions

$$\mu \geq 0, \qquad 3\lambda + 2\mu \geq 0, \tag{1.1.9}$$

are derived. For monoatomic gases, $3\lambda + 2\mu = 0$. This condition is usually used even in the case of more complicated gases.

1.1.7 *The energy equation*

The total energy is defined as

$$E = \rho(e + |\boldsymbol{v}|^2/2), \tag{1.1.10}$$

where e is the internal (specific) energy.

Energy equation has the form

$$\begin{aligned} &\frac{\partial E}{\partial t} + \operatorname{div}(E\boldsymbol{v}) \\ &= \rho \boldsymbol{f} \cdot \boldsymbol{v} + \operatorname{div}(\mathcal{T}\boldsymbol{v}) + \rho q - \operatorname{div} \mathbf{q}. \end{aligned} \tag{1.1.11}$$

For a *Newtonian fluid* we have

$$\begin{aligned} \frac{\partial E}{\partial t} + \operatorname{div}(E\boldsymbol{v}) = \rho \boldsymbol{f} \cdot \boldsymbol{v} - \operatorname{div}(p\boldsymbol{v}) + \operatorname{div}(\lambda \boldsymbol{v} \operatorname{div} \boldsymbol{v}) \\ + \operatorname{div}(2\mu \mathbb{D}(\boldsymbol{v})\boldsymbol{v}) + \rho q - \operatorname{div} \mathbf{q}. \end{aligned} \tag{1.1.12}$$

Here q is the density of heat sources and $\mathbf{q}$ is the heat flux, which depends on the temperature by Fourier's law:

$$\mathbf{q} = -k \nabla \theta. \tag{1.1.13}$$

Here $k \geq 0$ denotes the heat conduction coefficient.

1.1.8 *Thermodynamical relations*

In order to complete the conservation law system, additional equations derived in thermodynamics have to be included.

The absolute temperature θ, the density ρ and the pressure p are called the *state variables.* All these quantities are positive functions. The gas is characterized by the equation of state

$$p = p(\rho, \theta) \tag{1.1.14}$$

and the relation

$$e = e(\rho, \theta). \tag{1.1.15}$$

Here we shall consider the so-called *perfect gas* (also called ideal gas) whose state variables satisfy the equation of state in the form

$$p = R\, \theta\, \rho. \tag{1.1.16}$$

$R > 0$ is the *gas constant*, which can be expressed in the form

$$R = c_p - c_v, \tag{1.1.17}$$

where c_p and c_v denote the *specific heat at constant pressure* and the *specific heat at constant volume*, respectively. From experiments we know that $c_p > c_v$, so that $R > 0$. We shall consider c_p and c_v to be constant, which is assumed for

perfect gases. Experiments show that this is true for a relatively large range of temperature. The quantity

$$\gamma = \frac{c_p}{c_v} > 1 \tag{1.1.18}$$

is called the *Poisson adiabatic constant.* For example, for air, $\gamma = 1.4$.

The internal energy of a perfect gas is given by

$$e = c_v \theta. \tag{1.1.19}$$

1.1.9 *Entropy*

One of the important thermodynamical quantities is the entropy S, defined by the relation

$$\theta \, \mathrm{d}S = \mathrm{d}e + p \, \mathrm{d}V, \tag{1.1.20}$$

where $V = 1/\rho$ is the so-called specific volume. This identity is derived in thermodynamics under the assumption that the internal energy is a function of S and $V : e = e(S, V)$, which explains the meaning of the differentials in (1.1.20).

Theorem 1.3 *For a perfect gas we have*

$$\begin{aligned} S &= c_v \ln \frac{p/p_0}{(\rho/\rho_0)^\gamma} + \text{const} \\ &= c_v \ln \frac{\theta/\theta_0}{(\rho/\rho_0)^{\gamma-1}} + \text{const}, \end{aligned} \tag{1.1.21}$$

where p_0 and ρ_0 are fixed (reference) values of pressure and density, respectively, and $\theta_0 = p_0/(R\rho_0)$.

1.1.10 *The second law of thermodynamics*

In irreversible processes,

$$\mathrm{d}S \geq \frac{\delta Q}{\theta}, \tag{1.1.22}$$

where δQ is the heat transmitted to the system. The mathematical formulation reads:

$$\frac{\partial(\rho S)}{\partial t} + \operatorname{div}(\rho S \boldsymbol{v}) \geq \frac{\rho q}{\theta} - \operatorname{div}\left(\frac{\mathbf{q}}{\theta}\right). \tag{1.1.23}$$

(Of course, it needs mathematical interpretation – we consider it in the sense of distributions.)

1.1.11 *Adiabatic flow*

If there is no heat transmission and heat exchange between fluid volumes, we speak of adiabatic flow. Hence, in adiabatic flow the heat sources and heat flux are zero, so that $q = 0$, $\mathbf{q} = 0$ and $k = 0$.

It is known that heat conductivity and internal friction represent two faces of molecular transmission. Heat conductivity is related to the transmission of

molecular kinetic energy and internal friction is conditioned by the transmission of molecular momentum. Therefore, it makes sense to speak of adiabatic flow particularly in the case of inviscid gas.

Theorem 1.4 *If the quantities describing the flow are continuously differentiable, then in adiabatic flow of an inviscid perfect gas we have*

$$\frac{\partial(\rho S)}{\partial t} + \operatorname{div}(\rho S \boldsymbol{v}) = 0 \tag{1.1.24}$$

and

$$S = \text{const} \quad \textit{along the trajectory of any fluid particle,} \tag{1.1.25}$$

$$p = \kappa\rho^{\gamma} \quad \textit{along the trajectory of any fluid particle,} \tag{1.1.26}$$

where κ is a constant dependent on the trajectory considered.

If condition (1.1.25) is satisfied, then we speak of *isentropic* flow. If $S = \text{const}$ in the whole flow field, then the flow is called *homoentropic*.

1.1.12 *Barotropic flow*

We say that the flow is barotropic if the pressure can be expressed as a function of the density:

$$p = p(\rho). \tag{1.1.27}$$

This means that $p(x,t) = p(\rho(x,t))$ for all $(x,t) \in \mathcal{M}$, or, more briefly, $p = p \circ \rho$. We assume that

$$\begin{aligned} &p : (0,+\infty) \to (0,+\infty) \\ &\text{and there exists the continuous derivative} \\ &p' > 0 \text{ on } (0,+\infty). \end{aligned} \tag{1.1.28}$$

From (1.1.26) it follows that in *adiabatic barotropic flow of an inviscid perfect gas* we have the relation

$$p = \kappa\rho^{\gamma}, \tag{1.1.29}$$

the constant κ being common for the whole flow field. Thus, the flow is homoentropic.

1.1.13 *Speed of sound; Mach number*

A more general model than barotropic flow is obtained in thermodynamics under the assumption that the pressure is a function of the density and entropy: $p =$

$p(\rho, S)$, where p is a continuously differentiable function and $\partial p/\partial \rho > 0$. For example, for a perfect gas, in view of Theorem 1.3, we have

$$p = f(\rho, S) = \kappa \rho^{\gamma} \exp(S/c_v), \qquad \kappa = \text{const} > 0. \tag{1.1.30}$$

Let us introduce the quantity

$$a = \sqrt{\frac{\partial f}{\partial \rho}} \tag{1.1.31}$$

which has the dimension m s^{-1} of velocity and is called the *speed of sound.* This terminology is based on the fact that a represents the speed of propagation of pressure waves of small intensity.

A further important characteristic of gas flow is the *Mach number*

$$M = \frac{|\boldsymbol{v}|}{a} \tag{1.1.32}$$

(which is obviously a dimensionless quantity). We say that the flow is *subsonic* or *sonic* or *supersonic* at a point x and time t, if

$$M(x,t) < 1 \qquad \text{or} \qquad M(x,t) = 1 \qquad \text{or} \qquad M(x,t) > 1, \tag{1.1.33}$$

respectively.

2

FINITE VOLUME METHOD

2.1 Basic properties of the Euler equations

Let us consider *adiabatic flow of an inviscid perfect gas* in a bounded domain $\Omega \subset I\!R^N$ and time interval $(0,T)$ with $T > 0$. Here $N = 2$ or 3 for 2D or 3D flow, respectively. We neglect outer volume force and heat sources. Our goal is to solve numerically the Euler equations

$$\frac{\partial \boldsymbol{w}}{\partial t} + \sum_{s=1}^{N} \frac{\partial \boldsymbol{f}_s(\boldsymbol{w})}{\partial x_s} = 0 \quad \text{in } Q_T = \Omega \times (0,T) \tag{2.1.1}$$

(Q_T is called a space-time cylinder), equipped with the initial condition

$$\boldsymbol{w}(x,0) = \boldsymbol{w}^0(x), \quad x \in \Omega, \tag{2.1.2}$$

with a given vector function $\boldsymbol{w}^0$ and boundary conditions

$$B(\boldsymbol{w}(x,t)) = 0 \quad \text{for } (x,t) \in \partial\Omega \times (0,T). \tag{2.1.3}$$

Here B is a suitable boundary operator. The specification of the boundary conditions and their approximation will be given later (see Section 2.2.5). The state vector $\boldsymbol{w} = (\rho, \rho v_1, \dots, \rho v_N, E)^{\mathrm{T}} \in I\!R^m$, $m = N+2$ (i.e. $m = 4$ or 5 for 2D or 3D flow, respectively), the fluxes $\boldsymbol{f}_s$, $s = 1, \dots, N$, are m-dimensional mappings defined by

$$\begin{aligned}
\boldsymbol{f}_s(\boldsymbol{w}) &= (f_{s1}(\boldsymbol{w}), \dots, f_{sm}(\boldsymbol{w}))^{\mathrm{T}} \qquad (2.1.4)\\
&= (\rho v_s, \rho v_1 v_s + \delta_{1s} p, \dots, \rho v_N v_s + \delta_{Ns} p, (E+p)v_s)^{\mathrm{T}} \\
&= \Bigg(w_{s+1}, w_2 w_{s+1}/w_1 + \delta_{1s}(\gamma-1)\big(w_m - \sum_{i=2}^{m-1} w_i^2/(2w_1)\big), \dots, \\
&\quad w_{m-1} w_{s+1}/w_1 + \delta_{m-2,s}(\gamma-1)\big(w_m - \sum_{i=2}^{m-1} w_i^2/(2w_1)\big), \\
&\quad w_{s+1}\big(\gamma w_m - (\gamma-1)\sum_{i=2}^{m-1} w_i^2/(2w_1)\big)/w_1 \Bigg)^{\mathrm{T}}
\end{aligned}$$

is the *flux* of the quantity $\boldsymbol{w}$ in the direction x_s. Often, $\boldsymbol{f}_s$, $s = 1, \dots, N$, are called *inviscid Euler fluxes*. The domain of definition of the vector-valued functions $\boldsymbol{f}_s$ is

the open set $D \subset \mathbb{R}^m$ of vectors $\boldsymbol{w} = (w_1, \dots, w_m)^{\mathrm{T}}$ such that the corresponding density and pressure are positive:

$$D = \Big\{ \boldsymbol{w} \in \mathbb{R}^m; w_1 = \rho > 0,\ w_s = \rho v_{s-1} \in \mathbb{R} \text{ for } s = 2, \dots, m-1, \qquad (2.1.5)$$
$$w_m - \sum_{i=2}^{m-1} w_i^2/(2w_1) = p/(\gamma - 1) > 0 \Big\}.$$

Let us recall that for each $\boldsymbol{w} \in D$ and $\boldsymbol{n} = (n_1, \dots, n_N)^{\mathrm{T}} \in \mathbb{R}^N$ with $|\boldsymbol{n}| = 1$ the mapping

$$\boldsymbol{\mathcal{P}}(\boldsymbol{w}, \boldsymbol{n}) = \sum_{s=1}^{N} n_s \boldsymbol{f}_s(\boldsymbol{w}) \qquad (2.1.6)$$

has the Jacobi matrix

$$\mathbb{P}(\boldsymbol{w}, \boldsymbol{n}) = D\boldsymbol{\mathcal{P}}(\boldsymbol{w}, \boldsymbol{n})/D\boldsymbol{w} = \sum_{s=1}^{N} n_s \mathbb{A}_s(\boldsymbol{w}), \qquad (2.1.7)$$

with eigenvalues $\lambda_i = \lambda_i(\boldsymbol{w}, \boldsymbol{n})$:

$$\lambda_1 = \boldsymbol{v} \cdot \boldsymbol{n} - a, \quad \lambda_2 = \cdots = \lambda_{m-1} = \boldsymbol{v} \cdot \boldsymbol{n}, \quad \lambda_m = \boldsymbol{v} \cdot \boldsymbol{n} + a, \qquad (2.1.8)$$

where $\boldsymbol{v} = (v_1, \dots, v_N)^{\mathrm{T}}$ is the velocity and $a = \sqrt{\gamma p/\rho}$ is the speed of sound.

The matrix $\mathbb{P}(\boldsymbol{w}, \boldsymbol{n})$ is diagonalizable with the aid of the matrices $\mathrm{T} = \mathrm{T}(\boldsymbol{w}, \boldsymbol{n})$ and $\mathrm{T}^{-1} = \mathrm{T}^{-1}(\boldsymbol{w}, \boldsymbol{n})$:

$$\mathbb{P}(\boldsymbol{w}, \boldsymbol{n}) = \mathrm{T}\, \Lambda\!\!\backslash\, \mathrm{T}^{-1}, \quad \Lambda\!\!\backslash = \mathrm{diag}(\lambda_1, \dots, \lambda_m). \qquad (2.1.9)$$

The mapping $\boldsymbol{\mathcal{P}}(\boldsymbol{w}, \boldsymbol{n})$ is called the *flux of the quantity* $\boldsymbol{w}$ *in the direction* $\boldsymbol{n}$. The above results imply that the Euler equations form a *diagonally hyperbolic system.*

In the sequel, for simplicity we shall consider two-dimensional flow (i.e. $N = 2,\ m = 4$).

A further interesting property is the *rotational invariance* of the Euler equations, represented by the relations

$$\boldsymbol{\mathcal{P}}(\boldsymbol{w}, \boldsymbol{n}) = \sum_{s=1}^{2} \boldsymbol{f}_s(\boldsymbol{w}) n_s = \boldsymbol{Q}^{-1}(\boldsymbol{n}) \boldsymbol{f}_1(\boldsymbol{Q}(\boldsymbol{n})\boldsymbol{w}), \qquad (2.1.10)$$
$$\mathbb{P}(\boldsymbol{w}, \boldsymbol{n}) = \sum_{s=1}^{2} \mathbb{A}_s(\boldsymbol{w}) n_s = \boldsymbol{Q}^{-1}(\boldsymbol{n}) \mathbb{A}_1(\boldsymbol{Q}(\boldsymbol{n})\boldsymbol{w}) \boldsymbol{Q}(\boldsymbol{n}),$$
$$\boldsymbol{n} = (n_1, n_2) \in \mathbb{R}^2, |\boldsymbol{n}| = 1, \boldsymbol{w} \in D,$$

where

$$\boldsymbol{Q}(\boldsymbol{n}) = \begin{pmatrix} 1 & 0 & 0 & 0 \\ 0 & n_1 & n_2 & 0 \\ 0 & -n_2 & n_1 & 0 \\ 0 & 0 & 0 & 1 \end{pmatrix}. \tag{2.1.11}$$

This allows us to transform the Euler equations to the rotated coordinate system $\tilde{x}_1, \tilde{x}_2$ by

$$\begin{pmatrix} \tilde{x}_1 \\ \tilde{x}_2 \end{pmatrix} = \boldsymbol{Q}_0(\boldsymbol{n}) \begin{pmatrix} x_1 \\ x_2 \end{pmatrix} + \tilde{\sigma}, \tag{2.1.12}$$

where $\tilde{\sigma} \in I\!R^2$ and

$$\boldsymbol{Q}_0(\boldsymbol{n}) = \begin{pmatrix} n_1 & n_2 \\ -n_2 & n_1 \end{pmatrix}, \tag{2.1.13}$$

then the transformation of the state vector $\boldsymbol{w}$ yields the state vector

$$\boldsymbol{q} = \boldsymbol{Q}(\boldsymbol{n})\boldsymbol{w}. \tag{2.1.14}$$

We consider the transformed state vector $\boldsymbol{q}$ as a function of $\tilde{x} = (\tilde{x}_1, \tilde{x}_2)$ and time t:

$$\boldsymbol{q} = \boldsymbol{q}(\tilde{x}, t) = \boldsymbol{Q}(\boldsymbol{n})\boldsymbol{w}(\boldsymbol{Q}_0^{-1}(\boldsymbol{n})(\tilde{x} - \tilde{\sigma}), t). \tag{2.1.15}$$

Then the function $\boldsymbol{q} = \boldsymbol{q}(\tilde{x}, t)$ satisfies the transformed system of the Euler equations

$$\frac{\partial \boldsymbol{q}}{\partial t} + \sum_{s=1}^{2} \frac{\partial \boldsymbol{f}_s(\boldsymbol{q})}{\partial \tilde{x}_s} = 0. \tag{2.1.16}$$

Finally, let us note that fluxes $\boldsymbol{f}_s$ and $\boldsymbol{\mathcal{P}}$ *homogeneous mappings of order one*: e.g.,

$$\boldsymbol{f}_s(\alpha \boldsymbol{w}) = \alpha \boldsymbol{f}_s(\boldsymbol{w}), \quad \alpha > 0. \tag{2.1.17}$$

This implies that

$$\boldsymbol{f}_s(\boldsymbol{w}) = \mathbb{A}_s(\boldsymbol{w})\boldsymbol{w}. \tag{2.1.18}$$

Similar properties hold also for $N = 3$.

2.2 The finite volume method for the multidimensional Euler equations

Now let us deal with the finite volume (FV) discretization of system (2.1.1). The finite volume method is very popular in computational fluid dynamics, because it is robust, flexible, allows the solution of flow problems in domains with a complicated geometry and its algorithmization is simple. For a survey of various techniques and results from the FV method, we refer the reader to the excellent monograph (Eymard *et al.*, 2000). First we describe the construction of a finite volume mesh.

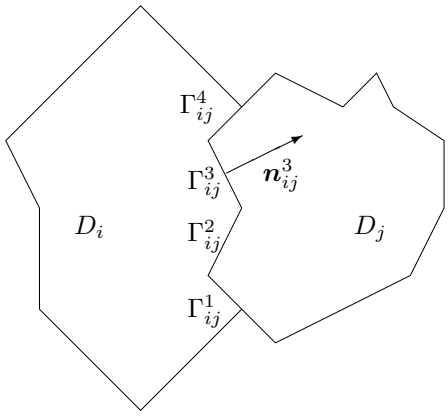

FIG. 2.1. Neighbouring finite volumes in 2D, $\Gamma_{ij} = \bigcup_{\alpha=1}^{4} \Gamma_{ij}^{\alpha}$

2.2.1 *Finite volume mesh*

Let $\Omega \subset I\!R^N$ be a domain occupied by the fluid. If $N = 2$, then by Ω_h we denote a polygonal approximation of Ω. This means that the boundary $\partial\Omega_h$ of Ω_h consists of a finite number of closed simple piecewise linear curves. For $N = 3$, Ω_h will denote a polyhedral approximation of Ω. The system $\mathcal{D}_h = \{D_i\}_{i\in J}$, where $J \subset Z^+ = \{0, 1, \ldots\}$ is an index set and $h > 0$, will be called a *finite volume mesh* in Ω_h, if D_i, $i \in J$, are *closed polygons* or *polyhedrons*, if $N = 2$ or 3, respectively, with mutually disjoint interiors such that

$$\overline{\Omega}_h = \bigcup_{i\in J} D_i. \tag{2.2.19}$$

The elements $D_i \in \mathcal{D}_h$ are called *finite volumes*. Two finite volumes D_i, $D_j \in \mathcal{D}_h$ are either disjoint or their intersection is formed by a common part of their boundaries ∂D_i and ∂D_j. If $\partial D_i \cap \partial D_j$ contains at least one straight segment, then we call D_i and D_j *neighbouring finite volumes* (or simply neighbours). For two neighbours D_i, $D_j \in \mathcal{D}_h$ we set

$$\Gamma_{ij} = \partial D_i \cap \partial D_j = \Gamma_{ji}. \tag{2.2.20}$$

Obviously, Γ_{ij} is formed by a finite number β_{ij} of straight segments $\Gamma_{ij}^{\alpha} = \Gamma_{ji}^{\alpha}$:

$$\Gamma_{ij} = \bigcup_{\alpha=1}^{\beta_{ij}} \Gamma_{ij}^{\alpha}. \tag{2.2.21}$$

See Fig. 2.1. We shall call Γ_{ij}^{α} *faces* of D_i.

Further, we introduce the following *notation*:

$$|D_i| = N\text{-dimensional measure of } D_i \tag{2.2.22}$$

$= \text{area of } D_i \text{ if } N = 2, \text{ or volume of } D_i \text{ if } N = 3,$

$|\Gamma_{ij}^{\alpha}| = (N-1)\text{-dimensional measure of } \Gamma_{ij}^{\alpha}$

$= \text{the length of } \Gamma_{ij}^{\alpha} \text{ if } N = 2, \text{ or area of } \Gamma_{ij}^{\alpha} \text{ if } N = 3,$

$\boldsymbol{n}_{ij}^{\alpha} = ((n_{ij}^{\alpha})_1, \ldots, (n_{ij}^{\alpha})_N)^{\mathrm{T}} = \text{unit outer normal to } \partial D_i \text{ on } \Gamma_{ij}^{\alpha},$

$h_i = \operatorname{diam}(D_i),$

$h = \sup_{i \in J} h_i,$

$|\partial D_i| = (N-1)\text{-dimensional measure of } \partial D_i,$

$s(i) = \{j \in J; j \neq i, D_j \text{ is a neighbour of } D_i\}.$

Clearly, $\boldsymbol{n}_{ij}^{\alpha} = -\boldsymbol{n}_{ji}^{\alpha}$.

The straight segments that form the intersections of $\partial\Omega_h$ with finite volumes D_i adjacent to $\partial\Omega_h$ will be denoted by S_j and numbered by negative indexes j forming an index set $J_B \subset Z^- = \{-1, -2, \ldots\}$. Hence, $J \cap J_B = \emptyset$ and $\partial\Omega_h = \bigcup_{j \in J_B} S_j$. For a finite volume D_i adjacent to the boundary $\partial\Omega_h$, i.e. if $S_j \subset \partial\Omega_h \cap \partial D_i$ for some $j \in J_B$, we set

$$\begin{aligned} &\gamma(i) = \{j \in J_B; S_j \subset \partial D_i \cap \partial\Omega_h\}, \\ &\Gamma_{ij} = \Gamma_{ij}^1 = S_j, \quad \beta_{ij} = 1 \quad \text{for } j \in \gamma(i). \end{aligned} \tag{2.2.23}$$

If D_i is not adjacent to $\partial\Omega_h$, then we put $\gamma(i) = \emptyset$. By $\boldsymbol{n}_{ij}^{\alpha}$ we again denote the unit outer normal to ∂D_i on Γ_{ij}^{α}. Then, putting

$$S(i) = s(i) \cup \gamma(i), \tag{2.2.24}$$

we have

$$\partial D_i = \bigcup_{j \in S(i)} \bigcup_{\alpha=1}^{\beta_{ij}} \Gamma_{ij}^{\alpha}, \tag{2.2.25}$$

$$\partial D_i \cap \partial\Omega_h = \bigcup_{j \in \gamma(i)} \bigcup_{\alpha=1}^{\beta_{ij}} \Gamma_{ij}^{\alpha},$$

$$|\partial D_i| = \sum_{j \in S(i)} \sum_{\alpha=1}^{\beta_{ij}} |\Gamma_{ij}^{\alpha}|.$$

2.2.1.1 *Finite volumes in 2D* In practical computations one uses several types of finite volume meshes:

a) *Triangular mesh* In this case $\mathcal{D}_h$ is a triangulation of the domain Ω_h with the usual properties from the finite element method (Ciarlet, 1979): $D_i \in \mathcal{D}_h$ are closed triangles satisfying conditions (2.2.19) and

$$\begin{aligned} &\text{if } D_i,\ D_j \in \mathcal{D}_h,\ D_i \neq D_j, \text{ then either } D_i \cap D_j = \emptyset \\ &\text{or } D_i \cap D_j \text{ is a common vertex of } D_i \text{ and } D_j \end{aligned} \tag{2.2.26}$$

or $D_i \cap D_j$ is a common side of D_i and D_j.

The triangulation satisfying (2.2.26) is called *conforming*. Then, under the above notation, Γ_{ij} consists of only one straight segment and, thus, we have $\beta_{ij} = 1$ and simply write $\partial D_i = \bigcup_{j \in S(i)} \Gamma_{ij}$.

b) *Quadrilateral mesh* Now $\mathcal{D}_h$ consists of closed convex quadrilaterals D_i.

c) *Dual finite volume mesh over a triangular grid*

d) *Barycentric finite volumes over a triangular grid*

2.2.2 *Derivation of a general finite volume scheme*

In order to derive a finite volume scheme, we can proceed in the following way. Let us assume that $\boldsymbol{w} : \overline{\Omega} \times [0,T] \to \mathbb{R}^m$ is a classical (i.e. C^1-) solution of system (2.1.1), $\mathcal{D}_h = \{D_i\}_{i \in J}$ is a finite volume mesh in a polyhedral approximation Ω_h of Ω. Let us construct a partition $0 = t_0 < t_1 < \dots$ of the time interval $[0,T]$ and denote by $\tau_k = t_{k+1} - t_k$ the time step between t_k and t_{k+1}. Integrating equation (2.1.1) over the set $D_i \times (t_k, t_{k+1})$ and using Green's theorem on D_i, we get the identity

$$\int_{D_i} \boldsymbol{w}(x,t)\,\mathrm{d}x \Big|_{t=t_k}^{t_{k+1}} + \int_{t_k}^{t_{k+1}} \left(\int_{\partial D_i} \sum_{s=1}^{N} \boldsymbol{f}_s(\boldsymbol{w}) n_s \,\mathrm{d}S \right) \mathrm{d}t = 0.$$

Moreover, taking into account (2.2.25), we can write

$$\begin{aligned} &\int_{D_i} (\boldsymbol{w}(x,t_{k+1}) - \boldsymbol{w}(x,t_k))\,\mathrm{d}x \qquad (2.2.27)\\ &\quad + \int_{t_k}^{t_{k+1}} \left(\sum_{j \in S(i)} \sum_{\alpha=1}^{\beta_{ij}} \int_{\Gamma_{ij}^\alpha} \sum_{s=1}^{N} \boldsymbol{f}_s(\boldsymbol{w}) n_s \,\mathrm{d}S \right) \mathrm{d}t = 0. \end{aligned}$$

Now we shall approximate the integral averages $\int_{D_i} \boldsymbol{w}(x,t_k)\mathrm{d}x/|D_i|$ of the quantity $\boldsymbol{w}$ over the finite volume D_i at time instant t_k by $\boldsymbol{w}_i^k$:

$$\boldsymbol{w}_i^k \approx \frac{1}{|D_i|} \int_{D_i} \boldsymbol{w}(x,t_k)\,\mathrm{d}x, \qquad (2.2.28)$$

called the value of *the approximate solution* on D_i at time t_k. Further, we approximate the flux $\sum_{s=1}^N \boldsymbol{f}_s(\boldsymbol{w})(n_{ij}^\alpha)_s$ of the quantity $\boldsymbol{w}$ through the face Γ_{ij}^α in the direction $\boldsymbol{n}_{ij}^\alpha$ with the aid of a *numerical flux* $\boldsymbol{H}(\boldsymbol{w}_i^\ell, \boldsymbol{w}_j^\ell, \boldsymbol{n}_{ij}^\alpha)$, depending on the value of the approximate solution $\boldsymbol{w}_i^\ell$ on the finite volume D_i, the value $\boldsymbol{w}_j^\ell$ on D_j, and on the normal $\boldsymbol{n}_{ij}^\alpha$ at suitable time instants t_ℓ:

$$\sum_{s=1}^{N} \boldsymbol{f}_s(\boldsymbol{w})(n_{ij}^\alpha)_s \approx \boldsymbol{H}(\boldsymbol{w}_i^\ell, \boldsymbol{w}_j^\ell, \boldsymbol{n}_{ij}^\alpha). \qquad (2.2.29)$$

We choose, for example, $\ell = k$ or $\ell = k+1$. If $\Gamma_{ij}^\alpha \subset \partial\Omega_h$ (i.e. the finite volume D_i is adjacent to $\partial\Omega_h$, $j \in \gamma(i)$, $\alpha = 1$ and $\Gamma_{ij}^1 = \Gamma_{ij}$), then there is no neighbour

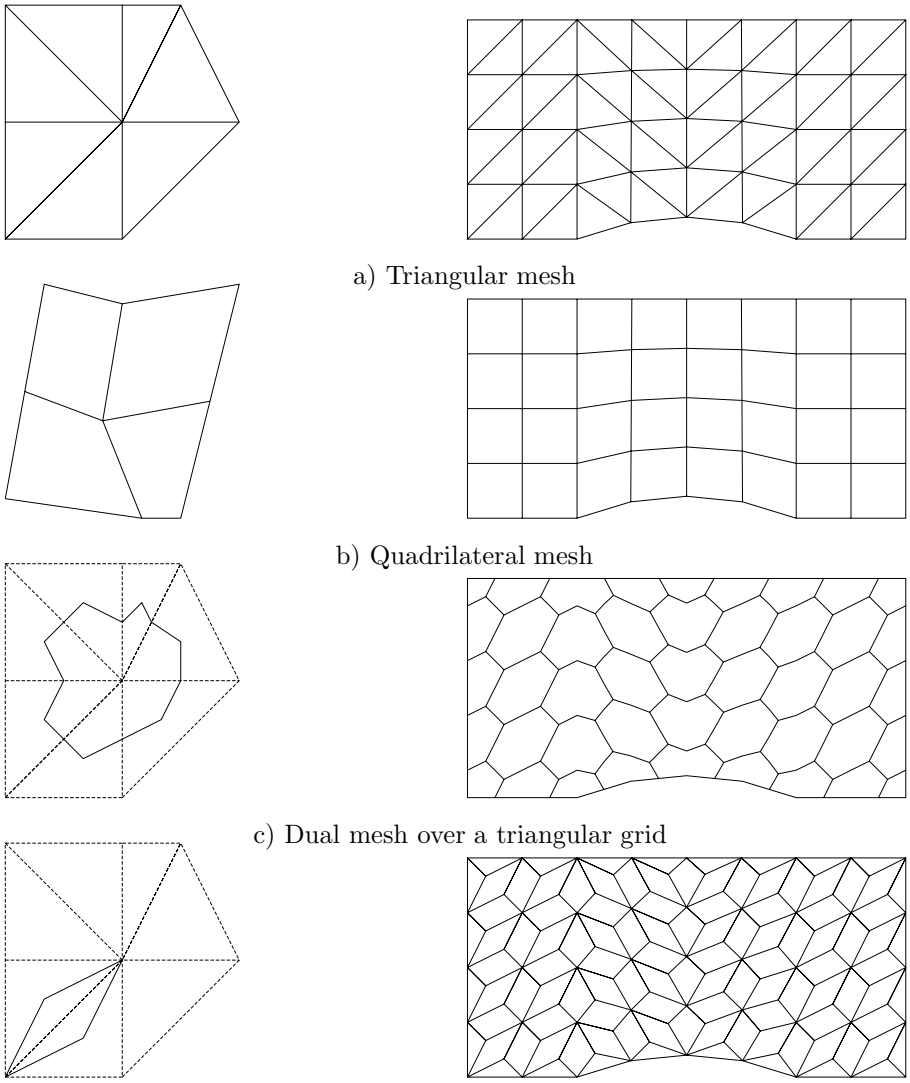

a) Triangular mesh

b) Quadrilateral mesh

c) Dual mesh over a triangular grid

d) Barycentric mesh over a triangular grid

FIG. 2.2. Finite volume meshes in 2D

D_j of D_i adjacent to the face Γ_{ij} from the exterior of Ω_h and it is necessary to specify $\boldsymbol{w}_j^\ell$ on the basis of boundary conditions – see Section 2.2.5. In such a way we arrive at the approximation

$$\int_{t_k}^{t_{k+1}} \left(\int_{\Gamma_{ij}^\alpha} \sum_{s=1}^{N} \boldsymbol{f}_s(\boldsymbol{w})(n_{ij}^\alpha)_s \, \mathrm{d}S \right) \mathrm{d}t \tag{2.2.30}$$
$$\approx \tau_k \boldsymbol{H}(\boldsymbol{w}_i^k, \boldsymbol{w}_j^k, \boldsymbol{n}_{ij}^\alpha)|\Gamma_{ij}^\alpha|.$$

Using (2.2.27), (2.2.28) and (2.2.30), we obtain the following *finite volume explicit scheme*: with $\vartheta = 0$:

$$\boldsymbol{w}_i^{k+1} = \boldsymbol{w}_i^k - \frac{\tau_k}{|D_i|} \sum_{j \in S(i)} \sum_{\alpha=1}^{\beta_{ij}} \boldsymbol{H}(\boldsymbol{w}_i^k, \boldsymbol{w}_j^k, \boldsymbol{n}_{ij}^\alpha)|\Gamma_{ij}^\alpha|, \tag{2.2.31}$$
$$D_i \in \mathcal{D}_h, \ t_k \in [0, T).$$

The FV method is equipped with *initial conditions* $\boldsymbol{w}_i^0, \ i \in J$, defined by

$$\boldsymbol{w}_i^0 = \frac{1}{|D_i|} \int_{D_i} \boldsymbol{w}^0(x) \, \mathrm{d}x, \tag{2.2.32}$$

under the assumption that the function $\boldsymbol{w}^0$ from (2.1.2) is locally integrable: $\boldsymbol{w}^0 \in L^1_{\mathrm{loc}}(\Omega)^m$.

2.2.3 *Properties of the numerical flux*

In what follows, we shall assume that the numerical flux $\boldsymbol{H}$ has the following properties:

1. $\boldsymbol{H}(\boldsymbol{u}, \boldsymbol{v}, \boldsymbol{n})$ is defined and continuous on $D \times D \times \mathcal{S}_1$, where D is the domain of definition of the fluxes $\boldsymbol{f}_s$ and $\mathcal{S}_1$ is the unit sphere in $\mathbb{R}^N$: $\mathcal{S}_1 = \{\boldsymbol{n} \in \mathbb{R}^N; |\boldsymbol{n}| = 1\}$.
2. $\boldsymbol{H}$ is *consistent*:

$$\boldsymbol{H}(\boldsymbol{u}, \boldsymbol{u}, \boldsymbol{n}) = \boldsymbol{\mathcal{P}}(\boldsymbol{u}, \boldsymbol{n}) = \sum_{s=1}^{N} \boldsymbol{f}_s(\boldsymbol{u}) n_s, \quad \boldsymbol{u} \in D, \ \boldsymbol{n} \in \mathcal{S}_1. \tag{2.2.33}$$

3. $\boldsymbol{H}$ is *conservative*:

$$\boldsymbol{H}(\boldsymbol{u}, \boldsymbol{v}, \boldsymbol{n}) = -\boldsymbol{H}(\boldsymbol{v}, \boldsymbol{u}, -\boldsymbol{n}), \quad \boldsymbol{u}, \boldsymbol{v} \in D, \ \boldsymbol{n} \in \mathcal{S}_1. \tag{2.2.34}$$

If $\boldsymbol{H}$ satisfies conditions (2.2.33) and (2.2.34), the *method* is called *consistent* and *conservative*, respectively. (Note that the conservativity of the scheme means that the flux from the finite volume D_i into D_j through Γ_{ij}^α has the same magnitude, but opposite sign, as the flux from D_j into D_i.)

2.2.4 *Construction of some numerical fluxes*

One possible way to construct a numerical flux $\boldsymbol{H}$ is to use an analogy with the 1D case, replacing the 1D flux $\boldsymbol{f}(\boldsymbol{w})$ by the N-dimensional flux $\boldsymbol{\mathcal{P}}(\boldsymbol{w}, \boldsymbol{n})$ in the direction $\boldsymbol{n} \in \mathcal{S}_1$ defined in (2.1.6). In this way we obtain the generalization

of the Lax–Friedrichs scheme and flux vector splitting schemes of the Godunov type

a) The *Lax–Friedrichs numerical flux* is defined by

$$\boldsymbol{H}_{\mathrm{LF}}(\boldsymbol{u},\boldsymbol{v},\boldsymbol{n}) = \frac{1}{2}\left(\boldsymbol{\mathcal{P}}(\boldsymbol{u},\boldsymbol{n}) + \boldsymbol{\mathcal{P}}(\boldsymbol{v},\boldsymbol{n}) - \frac{1}{\lambda}(\boldsymbol{v}-\boldsymbol{u})\right), \quad \boldsymbol{u},\boldsymbol{v}\in D,\ \boldsymbol{n}\in\mathcal{S}_1. \tag{2.2.35}$$

Here $\lambda > 0$ is independent of $\boldsymbol{u},\boldsymbol{v}$, but depends, in general, on Γ_{ij}^{α} in the scheme.

To obtain flux vector splitting schemes, we use relations (2.1.6)–(2.1.9). On the basis of (2.1.9) we define the matrices

$$\Lambda\!\!\backslash^{\pm} = \mathrm{diag}(\lambda_1^{\pm},\dots,\lambda_m^{\pm}), \quad |\Lambda\!\!\backslash| \;=\; \mathrm{diag}(|\lambda_1|,\dots,|\lambda_m|), \tag{2.2.36}$$

$$\mathbb{P}^{\pm} = \mathrm{T}\Lambda\!\!\backslash^{\pm}\mathrm{T}^{-1}, \quad |\mathbb{P}| \;=\; \mathrm{T}|\Lambda\!\!\backslash|\mathrm{T}^{-1}, \tag{2.2.37}$$

depending on $\boldsymbol{w}\in D$ and $\boldsymbol{n}\in\mathcal{S}_1$. Now we define the following schemes:

b) *The Steger–Warming scheme* has the numerical flux

$$\boldsymbol{H}_{\mathrm{SW}}(\boldsymbol{u},\boldsymbol{v},\boldsymbol{n}) = \mathbb{P}^{+}(\boldsymbol{u},\boldsymbol{n})\boldsymbol{u} + \mathbb{P}^{-}(\boldsymbol{v},\boldsymbol{n})\boldsymbol{v}, \quad \boldsymbol{u},\boldsymbol{v}\in D,\ \boldsymbol{n}\in\mathcal{S}_1. \tag{2.2.38}$$

c) *The Vijayasundaram scheme*:

$$\boldsymbol{H}_{\mathrm{V}}(\boldsymbol{u},\boldsymbol{v},\boldsymbol{n}) = \mathbb{P}^{+}\left(\frac{\boldsymbol{u}+\boldsymbol{v}}{2},\boldsymbol{n}\right)\boldsymbol{u} + \mathbb{P}^{-}\left(\frac{\boldsymbol{u}+\boldsymbol{v}}{2},\boldsymbol{n}\right)\boldsymbol{v}. \tag{2.2.39}$$

d) *The Van Leer scheme*:

$$\boldsymbol{H}_{\mathrm{VL}}(\boldsymbol{u},\boldsymbol{v},\boldsymbol{n}) = \frac{1}{2}\left\{\boldsymbol{\mathcal{P}}(\boldsymbol{u},\boldsymbol{n}) + \boldsymbol{\mathcal{P}}(\boldsymbol{v},\boldsymbol{n}) - \left|\mathbb{P}\left(\frac{\boldsymbol{u}+\boldsymbol{v}}{2},\boldsymbol{n}\right)\right|(\boldsymbol{v}-\boldsymbol{u})\right\}. \tag{2.2.40}$$

Other possibilities: Roe numerical flux, Osher-Solomon numerical flux, direct Riemann solver.

2.2.5 *Boundary conditions*

Let $D_i\in\mathcal{D}_h$ be a finite volume adjacent to the boundary $\partial\Omega_h$, i.e. ∂D_i is formed by faces $\Gamma = \Gamma_{ij}^1 \subset \partial\Omega_h$ ($j\in\gamma(i)$) and let $\boldsymbol{n} = \boldsymbol{n}_{ij}^1$ be a unit outer normal to ∂D_i on Γ. (See Section 2.2.1.) In order to be able to compute the numerical flux $\boldsymbol{H}(\boldsymbol{w}_i^k,\boldsymbol{w}_j^k,\boldsymbol{n})$, it is necessary to specify the value $\boldsymbol{w}_j^k$.

We introduce a new Cartesian coordinate system $\tilde{x}_1,\dots,\tilde{x}_N$ in $\mathbb{R}^N$ ($N = 2$ or 3) with origin at the centre of gravity of the face Γ, the coordinate $\tilde{x}_1$ oriented in the direction of the normal $\boldsymbol{n}$ and $\tilde{x}_2,\dots,\tilde{x}_N$ tangent to Γ. The Euler equations transformed into this coordinate system have the form (2.1.16). Now we shall consider only the influence of the states $\boldsymbol{w}_i^k,\boldsymbol{w}_j^k$, which can be treated by neglecting the tangential derivatives $\partial/\partial\tilde{x}_s$, $s>1$. We get the system

with one space variable $\tilde{x}_1$. Further, we linearize this system around the state $\boldsymbol{q}_i^k = \boldsymbol{Q}(\boldsymbol{n})\boldsymbol{w}_i^k$. As a result we obtain the linear system

$$\frac{\partial \boldsymbol{q}}{\partial t} + \mathbb{A}_1(\boldsymbol{q}_i^k)\frac{\partial \boldsymbol{q}}{\partial \tilde{x}_1} = 0, \tag{2.2.41}$$

which will be considered in the set $(-\infty, 0)\times(0,\infty)$ and equipped with the initial condition

$$\boldsymbol{q}(\tilde{x}_1, 0) = \boldsymbol{q}_i^k, \quad \tilde{x}_1 \in (-\infty, 0), \tag{2.2.42}$$

and the boundary condition

$$\boldsymbol{q}(0, t) = \boldsymbol{q}_j^k, \quad t > 0. \tag{2.2.43}$$

Our goal is to choose the boundary state $\boldsymbol{q}_j^k$ in such a way that the initial-boundary value problem (2.2.41)–(2.2.43) is well-posed, i.e. it has a unique solution. Then we set $\boldsymbol{w}_j^k := \boldsymbol{Q}(\boldsymbol{n})^{-1}\boldsymbol{q}_j^k$. The solution of (2.2.41) can be written in the form

$$\boldsymbol{q}(\tilde{x}_1, t) = \sum_{s=1}^{m} \mu_s(\tilde{x}_1, t)\boldsymbol{r}_s, \tag{2.2.44}$$

where $\boldsymbol{r}_s = \boldsymbol{r}_s(\boldsymbol{q}_i^k)$ are the eigenvectors of the matrix $\mathbb{A}_1(\boldsymbol{q}_i^k)$ corresponding to its eigenvalues $\tilde{\lambda}_s = \tilde{\lambda}_s(\boldsymbol{q}_i^k)$ and creating a basis in $\mathbb{R}^m$ ($m = 4$ for $N = 2$). Moreover,

$$\boldsymbol{q}_i^k = \sum_{s=1}^{m} \alpha_s \boldsymbol{r}_s, \quad \boldsymbol{q}_j^k = \sum_{s=1}^{m} \beta_s \boldsymbol{r}_s. \tag{2.2.45}$$

Substituting (2.2.44) into (2.2.41) and using the relation $\mathbb{A}_1(\boldsymbol{q}_i^k)\boldsymbol{r}_s = \tilde{\lambda}_s \boldsymbol{r}_s$, we find that problem (2.2.41)–(2.2.43) is equivalent to m mutually independent linear initial-boundary value scalar problems

$$\begin{aligned}
&\frac{\partial \mu_s}{\partial t} + \tilde{\lambda}_s \frac{\partial \mu_s}{\partial \tilde{x}_1} = 0 \quad \text{in } (-\infty, 0)\times(0,\infty), \\
&\mu_s(\tilde{x}_1, 0) = \alpha_s, \quad \tilde{x}_1 \in (-\infty, 0), \\
&\mu_s(0, t) = \beta_s, \quad t \in (0,\infty), \\
&s = 1, \ldots, m,
\end{aligned} \tag{2.2.46}$$

which can be solved by the method of characteristics. The solution is

$$\mu_s(\tilde{x}_1, t) = \begin{cases} \alpha_s, & \tilde{x}_1 - \tilde{\lambda}_s t < 0, \\ \\ \beta_s, & \tilde{x}_1 - \tilde{\lambda}_s t > 0. \end{cases} \tag{2.2.47}$$

The possible situations are shown in Fig. 2.3. From this it is clear that

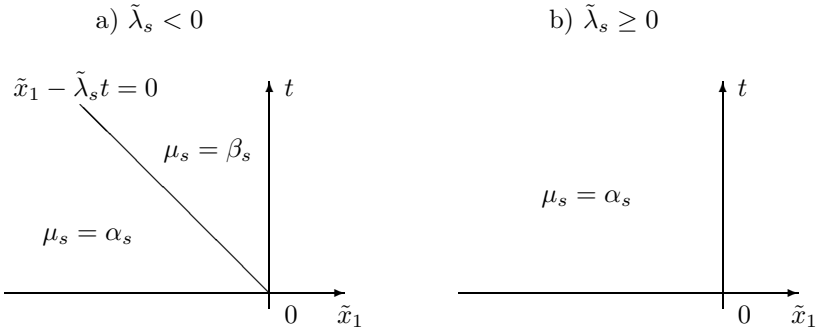

FIG. 2.3. Solution of problem (2.2.46)

if $\tilde{\lambda}_s > 0$, then $\beta_s = \alpha_s$ (β_s is not prescribed, but it is obtained by the extrapolation of μ_s to the boundary $\tilde{x}_1 = 0$);
if $\tilde{\lambda}_s = 0$, then β_s is not prescribed (but can again be defined as $\beta_s = \alpha_s$ by the continuous extension of μ_s to the boundary $\tilde{x}_1 = 0$);
if $\tilde{\lambda}_s < 0$, then β_s must be prescribed. (2.2.48)

We have

$$\tilde{\lambda}_s(\boldsymbol{q}_i^k) = \lambda_s(\boldsymbol{w}_i^k, \boldsymbol{n}), \quad s = 1, \ldots, m, \tag{2.2.49}$$

where $\lambda_s(\boldsymbol{w}_i^k, \boldsymbol{n})$ are the eigenvalues of the Jacobi matrix $\mathbb{P}(\boldsymbol{w}_i^k, \boldsymbol{n})$ (see (2.1.7)–(2.1.8)). Hence, on the basis of the above considerations, we come to the following *conclusion.* On $\Gamma = \Gamma_{ij}^{\alpha} \subset \partial\Omega_h$ (i.e. $i \in J, j \in \gamma(i), \alpha = 1$) with normal $\boldsymbol{n} = \boldsymbol{n}_{ij}^{\alpha}$, pointing from D_i into D_j, we have to prescribe n_{pr} quantities characterizing the state vector $\boldsymbol{w}$, where n_{pr} is the number of negative eigenvalues of the matrix $\mathbb{P}(\boldsymbol{w}_i^k, \boldsymbol{n})$, whereas we extrapolate n_{ex} quantities to the boundary, where n_{ex} is the number of nonnegative eigenvalues of $\mathbb{P}(\boldsymbol{w}_i^k, \boldsymbol{n})$. The *extrapolation* of a quantity q to the boundary means in this case to set $q_j^k := q_i^k$. On the other hand, if we prescribe the boundary value of q, we set $q_j^k := q_{Bj}^k$ with a given value q_{Bj}^k, determined by the user on the basis of the physical character of the flow.

It is suitable to use a special treatment if Γ is a part of a *solid impermeable wall*, where $\boldsymbol{v} \cdot \boldsymbol{n} = 0$. Then the flux $\boldsymbol{\mathcal{P}}(\boldsymbol{w}, \boldsymbol{n})$ has the form

$$\begin{aligned} \boldsymbol{\mathcal{P}}(\boldsymbol{w}, \boldsymbol{n}) &= \sum_{s=1}^{N} \boldsymbol{f}_s(\boldsymbol{w}) n_s \\ &= (\boldsymbol{v} \cdot \boldsymbol{n})\boldsymbol{w} + p(0, n_1, \ldots, n_N, \boldsymbol{v} \cdot \boldsymbol{n})^{\mathrm{T}} \end{aligned} \tag{2.2.50}$$

Table 2.1 *Boundary conditions for 2D flow*

Type of boundary	Character of the flow	The sign of eigenvalues n_{pr} and n_{ex}	Quantities extrapolated	Quantities prescribed
INLET $(\boldsymbol{v}\cdot\boldsymbol{n}<0)$	supersonic flow $(-\boldsymbol{v}\cdot\boldsymbol{n}>a)$	$\lambda_1<0$ $\lambda_2=\lambda_3<0$ $\lambda_4<0$ $n_{pr}=4,\ n_{ex}=0$	—	ρ, v_1, v_2, p
	subsonic flow $(-\boldsymbol{v}\cdot\boldsymbol{n}\le a)$	$\lambda_1<0$ $\lambda_2=\lambda_3<0$ $\lambda_4\ge 0$ $n_{pr}=3,\ n_{ex}=1$	p	ρ, v_1, v_2
OUTLET $(\boldsymbol{v}\cdot\boldsymbol{n}>0)$	supersonic flow $(\boldsymbol{v}\cdot\boldsymbol{n}\ge a)$	$\lambda_1\ge 0$ $\lambda_2=\lambda_3>0$ $\lambda_4>0$ $n_{pr}=0,\ n_{ex}=4$	ρ, v_1, v_2, p	—
	subsonic flow $(\boldsymbol{v}\cdot\boldsymbol{n}<a)$	$\lambda_1<0$ $\lambda_2=\lambda_3>0$ $\lambda_4>0$ $n_{pr}=1,\ n_{ex}=3$	ρ, v_1, v_2	p
SOLID IMPER-MEABLE BOUNDARY	$\boldsymbol{v}\cdot\boldsymbol{n}=0$	$\lambda_1<0$ $\lambda_2=\lambda_3=0$ $\lambda_4>0$ $n_{pr}=1,\ n_{ex}=3$	p (ρ, v_t)	$\boldsymbol{v}\cdot\boldsymbol{n}=0$

$$= p(0, n_1, \dots, n_N, 0)^{\mathrm{T}},$$

which is uniquely determined on Γ by the extrapolated value of the pressure, i.e. by $p_j^k := p_i^k$. Therefore, on the part Γ of the impermeable solid boundary we define the numerical flux

$$\boldsymbol{H}(\boldsymbol{w}_i^k, \boldsymbol{w}_j^k, \boldsymbol{n}) = p_i^k(0, n_1, \dots, n_N, 0)^{\mathrm{T}}. \tag{2.2.51}$$

We can see that in view of (2.1.8), on an impermeable boundary, N eigenvalues $\lambda_2, \dots, \lambda_{m-1}$ of the matrix $\mathbb{P}(\boldsymbol{w}_i^k, \boldsymbol{n})$ are zero, the eigenvalue λ_1 is negative and the eigenvalue λ_m is positive. We prescribe one scalar quantity, namely $\boldsymbol{v}\cdot\boldsymbol{n}=0$, and extrapolate the pressure p (and possibly the density and tangential components to Γ of the velocity, i.e. we extrapolate $n_{ex}=m-1$ quantities).

There are several ways to choose what quantities should be prescribed or extrapolated. We present here one possibility, which is often used in practical computations. It is suitable to distinguish several cases given in Table 2.1 (for 2D flow, $N=2,\ m=4$).

In some technically relevant problems it is necessary to apply also boundary conditions of other types, such as periodic boundary conditions.

2.2.6 *Stability of the finite volume schemes*

Let $\mathbf{w}^k = \{\boldsymbol{w}_i^k\}_{i\in J}$ be an approximate solution on the k-th time level obtained with the aid of the finite volume method. By $\|\mathbf{w}^k\|$ we denote a norm of the approximation $\mathbf{w}^k$. We call the *scheme stable*, if there exists a constant $c > 0$ independent of τ, h, k such that

$$\|\mathbf{w}^k\| \le c\|\mathbf{w}^0\|, \quad k = 0, 1, \dots. \tag{2.2.52}$$

Usually an analogy to the L^p-norm ($p \in [1, \infty]$) is used:

$$\|\mathbf{w}^k\|_\infty = \sup_{i\in J} |\boldsymbol{w}_i^k|, \tag{2.2.53}$$

$$\|\mathbf{w}^k\|_p = \left\{ \sum_{i\in J} |D_i| |\boldsymbol{w}_i^k|^p \right\}^{1/p}, \quad p \in [1, \infty).$$

In what follows we shall be concerned with the stability of the *explicit* FV method (2.2.31). For simplicity we confine our considerations to the 2D case.

2.2.7 *Simplified scalar problem*

The analysis of the stability of finite volume schemes is rather difficult. Unfortunately, the von Neumann method cannot be used on irregular unstructured meshes. Some knowledge about the qualitative properties of some numerical method can be obtained, if it is applied to the *scalar Cauchy problem*

$$\begin{aligned} &\frac{\partial w}{\partial t} + \sum_{s=1}^{N} \frac{\partial f_s(w)}{\partial x_s} = 0 \quad \text{in } I\!R^N \times (0, \infty), \\ &w(x, 0) = w^0(x), \quad x \in I\!R^N. \end{aligned} \tag{2.2.54}$$

In this case $w : I\!R^N \times (0, \infty) \to I\!R$, $f_s \in C^1(I\!R)$. The explicit FV scheme now has the form

$$\begin{aligned} w_i^{k+1} &= w_i^k - \frac{\tau}{|D_i|} \sum_{j\in S(i)} \sum_{\alpha=1}^{\beta_{ij}} H(w_i^k, w_j^k, \boldsymbol{n}_{ij}) |\Gamma_{ij}^\alpha|, \quad i \in J, \\ w_i^0 &= \frac{1}{|D_i|} \int_{D_i} w^0(x)\, \mathrm{d}x, \quad i \in J \end{aligned} \tag{2.2.55}$$

(provided $w^0 \in L^1_{\mathrm{loc}}(I\!R^N)$). We assume that the numerical flux $H = H(u, v, \boldsymbol{n}) : I\!R^2 \times \mathcal{S}_1 \to I\!R$ has the properties from Section 2.2.3. Moreover, we shall use a stronger continuity assumption: let H be *locally Lipschitz-continuous*. This means that if $M > 0$, then there exists a constant $c(M) > 0$ such that

$$\begin{aligned} &|H(u, v, \boldsymbol{n}) - H(u^*, v^*, \boldsymbol{n})| \le c(M)(|u - u^*| + |v - v^*|), \\ &u, u^*, v, v^* \in [-M, M], \ \boldsymbol{n} \in \mathcal{S}_1. \end{aligned} \tag{2.2.56}$$

The concept of *monotonicity* plays an important role in the study of stability and convergence of scheme (2.2.55).

Definition 2.1 *Let $M > 0$. We say that the numerical flux H is monotone in the set $[-M, M]$, if the function '$u, v \in [-M, M]$, $\boldsymbol{n} \in \mathcal{S}_1 \to H(u, v, \boldsymbol{n}) \in \mathbb{R}$' is nonincreasing with respect to the second variable v. Thus, $H(u, v, \boldsymbol{n}) \leq H(u, \tilde{v}, \boldsymbol{n})$, provided $u, v, \tilde{v} \in [-M, M], v \geq \tilde{v}, \boldsymbol{n} \in \mathcal{S}_1$.*

It is easy to see that the monotone conservative numerical flux $H = H(u, v, \boldsymbol{n})$ is nondecreasing with respect to the first variable u. Let us recall the notation $\mathrm{w}^k = \{w_i^k\}_{i \in J}$ for the numerical solution at time t_k. We shall show that the monotonicity of the numerical flux implies the stability. Let us use the notation $\mathrm{w}^k = \{w_i^k\}_{i \in J}$ for the numerical solution at time t_k.

Theorem 2.2 *Let $M > 0$ and*

$$\mathrm{w}^0 \in \mathcal{M}_M = \{\mathrm{w} = \{w_j\}_{j \in J}; \|\mathrm{w}\|_\infty := \sup_{j \in J} |w_j| \leq M\}. \tag{2.2.57}$$

Let the following conditions be satisfied:

a) (2.2.56) *holds,*

b) H is consistent (i.e. (2.2.33) *holds),*

c) H is monotone in $[-M, M]$,

d) the stability condition

$$\tau c(M) |\partial D_i| / |D_i| \leq 1, \quad i \in J \tag{2.2.58}$$

is satisfied.

Then scheme (2.2.55) *is L^∞-stable:*

$$\|\mathrm{w}^k\|_\infty \leq \|\mathrm{w}^0\|_\infty \quad \forall k \in Z^+. \tag{2.2.59}$$

Proof By induction with respect to k we prove that

$$\text{a)} \quad \|\mathrm{w}^k\|_\infty \leq M, \qquad \text{b)} \quad \|\mathrm{w}^{k+1}\|_\infty \leq \|\mathrm{w}^k\|_\infty, \qquad k \in Z^+. \tag{2.2.60}$$

This already implies (2.2.59). Inequality (2.2.60), a) holds for $k = 0$. Let us assume it is true for some $k \geq 0$. Then we shall establish (2.2.60), b) and, thus, (2.2.60), a) for $k + 1$. Using the consistency (2.2.33) and Green's theorem, we find that for each $i \in J$,

$$\sum_{j \in S(i)} \sum_{\alpha=1}^{\beta_{ij}} H(w_i^k, w_i^k, \boldsymbol{n}_{ij}^\alpha) |\Gamma_{ij}^\alpha| = \sum_{j \in S(i)} \sum_{\alpha=1}^{\beta_{ij}} \left(\sum_{s=1}^N f_s(w_i^k) (n_{ij}^\alpha)_s \right) |\Gamma_{ij}^\alpha| \tag{2.2.61}$$

$$= \sum_{s=1}^N f_s(w_i^k) \left(\sum_{j \in S(i)} \sum_{\alpha=1}^{\beta_{ij}} (n_{ij}^\alpha)_s |\Gamma_{ij}^\alpha| \right) = \sum_{s=1}^N f_s(w_i^k) \int_{\partial D_i} n_s \, \mathrm{d}S$$

$$= \sum_{s=1}^{N} f_s(w_i^k) \int_{D_i} \frac{\partial 1}{\partial x_s}\, \mathrm{d}x = 0.$$

By virtue of (2.2.61), formula (2.2.55) can be rewritten in the form

$$\begin{aligned} w_i^{k+1} &= w_i^k - \frac{\tau}{|D_i|} \sum_{j\in S(i)} \sum_{\alpha=1}^{\beta_{ij}} \left(H(w_i^k, w_j^k, \boldsymbol{n}_{ij}^\alpha) - H(w_i^k, w_i^k, \boldsymbol{n}_{ij}^\alpha) \right) |\Gamma_{ij}^\alpha| \\ &= w_i^k - \frac{\tau}{|D_i|} \sum_{j\in S(i)} \sum_{\alpha=1}^{\beta_{ij}} \mathcal{H}_{ij}^\alpha |\Gamma_{ij}^\alpha| (w_i^k - w_j^k), \end{aligned}$$

where

$$\mathcal{H}_{ij}^\alpha = \begin{cases} \frac{H(w_i^k, w_j^k, \boldsymbol{n}_{ij}^\alpha) - H(w_i^k, w_i^k, \boldsymbol{n}_{ij}^\alpha)}{w_i^k - w_j^k}, & \text{if } w_j^k \neq w_i^k, \\ 0, & \text{if } w_j^k = w_i^k. \end{cases} \tag{2.2.62}$$

Hence,

$$w_i^{k+1} = \left(1 - \frac{\tau}{|D_i|} \sum_{j\in S(i)} \sum_{\alpha=1}^{\beta_{ij}} \mathcal{H}_{ij}^\alpha |\Gamma_{ij}^\alpha| \right) w_i^k + \frac{\tau}{|D_i|} \sum_{j\in S(i)} \sum_{\alpha=1}^{\beta_{ij}} \mathcal{H}_{ij}^\alpha |\Gamma_{ij}^\alpha| w_j^k. \tag{2.2.63}$$

From the monotonicity of H it follows that $\mathcal{H}_{ij}^\alpha \geq 0$. Moreover, by (2.2.62) and the Lipschitz-continuity of H in $[-M, M]$, we have $\mathcal{H}_{ij}^\alpha \leq c(M)$. From this and the stability condition (2.2.58) we get

$$\begin{aligned} &1 - \frac{\tau}{|D_i|} \sum_{j\in S(i)} \sum_{\alpha=1}^{\beta_{ij}} \mathcal{H}_{ij}^\alpha |\Gamma_{ij}^\alpha| \geq 1 - \frac{\tau c(M)}{|D_i|} \sum_{j\in S(i)} \sum_{\alpha=1}^{\beta_{ij}} |\Gamma_{ij}^\alpha| \qquad (2.2.64) \\ &= 1 - \tau c(M) |\partial D_i| / |D_i| \geq 0. \end{aligned}$$

These results now immediately imply that

$$\begin{aligned} |w_i^{k+1}| \leq &\left(1 - \frac{\tau}{|D_i|} \sum_{j\in S(i)} \sum_{\alpha=1}^{\beta_{ij}} \mathcal{H}_{ij}^\alpha |\Gamma_{ij}^\alpha| \right) |w_i^k| \\ &+ \frac{\tau}{|D_i|} \sum_{j\in S(i)} \sum_{\alpha=1}^{\beta_{ij}} \mathcal{H}_{ij}^\alpha |\Gamma_{ij}^\alpha| |w_j^k| \leq \|\mathrm{w}^k\|_\infty, \quad i \in J, \end{aligned}$$

which we wanted to prove. □

Now we come to the question of how to extend the above results to the upwind flux vector splitting schemes of the Godunov type for the solution of the Euler equations. The Vijayasundaram and Steger–Warming schemes applied to

the scalar equation (2.2.54) are consistent only in the case that this equation is linear:

$$\frac{\partial w}{\partial t} + \sum_{s=1}^{N} a_s \frac{\partial w}{\partial x_s} = 0, \tag{2.2.65}$$

where $a_s \in I\!R$. Let us denote $\boldsymbol{a} = (a_1, \ldots, a_N)^{\mathrm{T}}$. It is easy to see that the Vijayasundaram, Steger–Warming and Van Leer schemes applied to equation (2.2.65) become identical. The flux of the quantity w has the form

$$\mathcal{P}(w, \boldsymbol{n}) = w \sum_{s=1}^{N} a_s n_s = w(\boldsymbol{a} \cdot \boldsymbol{n}), \quad \boldsymbol{n} = (n_1, \ldots, n_N)^{\mathrm{T}} \in \mathcal{S}_1, \ w \in I\!R,$$

and the corresponding numerical flux becomes

$$H(u, v, \boldsymbol{n}) = (\boldsymbol{a} \cdot \boldsymbol{n})^{+} u + (\boldsymbol{a} \cdot \boldsymbol{n})^{-} v, \quad u, v \in I\!R, \quad \boldsymbol{n} \in \mathcal{S}_1. \tag{2.2.66}$$

We immediately see that this flux is monotone and Lipschitz-continuous with a constant $c(M) = |\boldsymbol{a}|$ for each $M > 0$. Then by virtue of Theorem 2.2, the Vijayasundaram, Steger–Warming and Van Leer schemes applied to equation (2.2.65) are stable under the *stability condition*

$$\tau |\boldsymbol{a}| |\partial D_i| / |D_i| \leq 1, \quad i \in J. \tag{2.2.67}$$

2.2.8 *Extension of the stability conditions to the Euler equations*

In the above example, the vector $\boldsymbol{a}$ represents the characteristic speed of propagation of disturbances in the quantity w. For the Euler equations, we can consider 4 characteristic directions (in the 2D case) given by the eigenvectors of the matrix $\mathbb{P}(\boldsymbol{w}, \boldsymbol{n})$ and the characteristic speeds are given by the corresponding eigenvalues $\lambda_s(\boldsymbol{w}, \boldsymbol{n}), \ s = 1, \ldots, 4$. We generalize the stability condition (2.2.67) to the Euler equations in such a way that the speed $|\boldsymbol{a}|$ is replaced by the magnitudes of the eigenvalues $\lambda_s(\boldsymbol{w}, \boldsymbol{n}), s = 1, \ldots, 4$. In this heuristic way we arrive at the CFL-stability condition of the form

$$\tau_k \lambda_{i,\max} |\partial D_i| / |D_i| \leq CFL, \quad i \in J, \tag{2.2.68}$$

where

$$\lambda_{i,\max}^{k} = \max_{\substack{r=1,\ldots,m, j \in S(i) \\ \alpha=1,\ldots,\beta_{ij}}} \left| \lambda_r(\boldsymbol{w}_i^k, \boldsymbol{n}_{ij}^{\alpha}) \right|. \tag{2.2.69}$$

Usually we choose CFL < 1, e.g. CFL=0.85.

3

FINITE ELEMENT METHODS

3.1 Combined finite volume–finite element method for viscous compressible flow

The finite volume method (FVM) represents an efficient and robust method for the solution of inviscid compressible flow. On the other hand, it is well-known that the finite element method (FEM) is suitable for the approximation of elliptic or parabolic problems. The use of advantages of both FE and FV techniques leads us to the *combined FV - FE method*. It is applied in such a way that the FVM is used for the discretization of inviscid Euler fluxes, whereas the FEM is applied to the approximation of viscous terms. This idea was proposed in (Feistauer *et al.*, 1995) and then further developed in (Feistauer *et al.*, 1997), (Feistauer *et al.*, 1999*a*), (Feistauer *et al.*, 1999*b*), (Angot *et al.*, 1998) (Dolejší *et al.*, 2002). For numerical computations of viscous flow, see, e.g. (Feistauer *et al.*, 1996), (Feistauer and Felcman, 1997), (Dolejší *et al.*, 2002).

For simplicity we assume that volume force and heat sources are equal to zero. Then the complete system describing viscous compressible flow in a domain $\Omega \subset \mathbb{R}^N$ with Lipschitz-continuous boundary $\Gamma = \partial\Omega$ and in a time interval $(0,T)$ can be written in the form

$$\frac{\partial \boldsymbol{w}}{\partial t} + \sum_{i=1}^{N} \frac{\partial \boldsymbol{f}_i(\boldsymbol{w})}{\partial x_i} = \sum_{i=1}^{N} \frac{\partial \boldsymbol{R}_i(\boldsymbol{w}, \nabla \boldsymbol{w})}{\partial x_i} \quad \text{in } Q_T, \tag{3.1.1}$$

where $Q_T = \Omega \times (0,T)$ and

$$\begin{aligned} \boldsymbol{w} &= (\rho, \rho v_1, \dots, \rho v_N, E)^{\mathrm{T}} \in \mathbb{R}^m, \\ m &= N+2, \ \boldsymbol{w} = \boldsymbol{w}(x,t), \ x \in \Omega, \ t \in (0,T), \\ \boldsymbol{f}_i(\boldsymbol{w}) &= (f_{i1}, \dots, f_{im})^{\mathrm{T}} \\ &= (\rho v_i, \rho v_1 v_i + \delta_{1i} p, \dots, \rho v_N v_i + \delta_{Ni} p, (E+p) v_i)^{\mathrm{T}} \\ \boldsymbol{R}_i(\boldsymbol{w}, \nabla \boldsymbol{w}) &= (R_{i1}, \dots, R_{im})^{\mathrm{T}} \\ &= (0, \tau_{i1}, \dots, \tau_{iN}, \tau_{i1} v_1 + \dots + \tau_{iN} v_N + k \partial\theta/\partial x_i)^{\mathrm{T}}, \\ \tau_{ij} &= \lambda \operatorname{div} \boldsymbol{v} \delta_{ij} + 2\mu d_{ij}(\boldsymbol{v}), \ d_{ij}(\boldsymbol{v}) = \frac{1}{2}\left(\frac{\partial v_i}{\partial x_j} + \frac{\partial v_j}{\partial x_i}\right). \end{aligned} \tag{3.1.2, 3.1.3}$$

To system (3.1.1) we add the thermodynamical relations valid for a *perfect gas*:

$$p = (\gamma - 1)(E - \rho|\boldsymbol{v}|^2/2), \quad \theta = \left(\frac{E}{\rho} - \frac{1}{2}|\boldsymbol{v}|^2\right)/c_v. \tag{3.1.4}$$

As usual, we use the following *notation*: $\boldsymbol{v} = (v_1, \dots, v_N)^{\mathrm{T}}$ – velocity vector, ρ – density, p – pressure, θ – absolute temperature, E – total energy, γ – Poisson adiabatic constant, c_v – specific heat at constant volume, μ, λ – viscosity coefficients, k – heat conduction coefficient. We assume $\mu, k > 0$, $2\mu + 3\lambda \geq 0$. Usually we set $\lambda = -2\mu/3$. By τ_{ij} we denote here the of the viscous part of the stress tensor.

The system is equipped with *initial conditions* written in the form

$$\boldsymbol{w}(x, 0) = \boldsymbol{w}^0(x), \quad x \in \Omega, \tag{3.1.5}$$

where $\boldsymbol{w}^0(x)$ is a given vector-valued function defined in Ω.

3.1.0.1 *Boundary conditions* The choice of appropriate boundary conditions represents an important problem in CFD. Boundary conditions have to reflect physical behaviour of the flow on the boundary of the domain occupied by the fluid on one hand, and should be in agreement with the character of partial differential equations on the other hand. There are several approaches to the formulation of the boundary conditions, depending on the problem and the geometry of the domain Ω.

In what follows, let us assume that Ω is a bounded domain. (In the flow past profiles their exterior is replaced by a bounded, sufficiently large domain Ω with boundary formed by the profiles and an artificial exterior component.) We write $\partial\Omega = \Gamma_I \cup \Gamma_O \cup \Gamma_W$, where Γ_I represents the inlet through which the gas enters the domain Ω, Γ_O is the outlet through which the gas should leave Ω and Γ_W represents impermeable fixed walls.

On Γ_I one can prescribe the conditions

$$\begin{aligned} &\text{a)}\ \ \rho\big|_{\Gamma_I \times (0,T)} = \rho_D, \quad \text{b)} \quad \boldsymbol{v}\big|_{\Gamma_I \times (0,T)} = \boldsymbol{v}_D = (v_{D1}, \dots, v_{DN})^{\mathrm{T}}, \\ &\text{c)}\ \ \theta\big|_{\Gamma_I \times (0,T)} = \theta_D \end{aligned} \tag{3.1.6}$$

with given functions $\rho_D, \boldsymbol{v}_D, \theta_D$. The inlet Γ_I is characterized, of course, by the condition $\boldsymbol{v}_D \cdot \boldsymbol{n} < 0$ on Γ_I, where $\boldsymbol{n}$ is the unit outer normal to $\partial\Omega$.

On Γ_W we use the no-slip boundary conditions. Moreover, we use here the *condition of adiabatic wall* with zero heat flux. Hence,

$$\begin{aligned} &\text{a)}\ \ \boldsymbol{v}\big|_{\Gamma_W \times (0,T)} = 0, \\ &\text{b)}\ \ \frac{\partial \theta}{\partial n}\Big|_{\Gamma_W \times (0,T)} = 0. \end{aligned} \tag{3.1.7}$$

The Dirichlet boundary conditions can be expressed in terms of the conservative variables in the form

$$\begin{aligned} w_1 = \rho_D,\ (w_2, \dots, w_{m-1})^{\mathrm{T}} = \rho_D \boldsymbol{v}_D, w_m = E_D \quad &\text{on } \Gamma_I \times (0,T), \\ w_2 = \dots = w_{m-1} = 0 \quad &\text{on } \Gamma_W \times (0,T). \end{aligned} \tag{3.1.8}$$

This is reflected in the definition of the *space of test functions*

$$\boldsymbol{V} = \big\{\boldsymbol{\varphi} = (\varphi_1, \dots, \varphi_m)^{\mathrm{T}}; \varphi_i \in H^1(\Omega),\ i = 1, \dots, m, \tag{3.1.9}$$

$$\varphi_1, \varphi_2, \dots, \varphi_m = 0 \text{ on } \Gamma_I,\ \varphi_2, \dots, \varphi_{m-1} = 0 \text{ on } \Gamma_W \big\}.$$

Now, assuming that $\boldsymbol{w}$ is a classical solution of problem (CFP), we multiply equation (3.1.1) by any $\boldsymbol{\varphi} \in \boldsymbol{V}$, integrate over Ω and apply Green's theorem to viscous terms. We obtain the identity

$$\begin{aligned} &\int_\Omega \frac{\partial \boldsymbol{w}}{\partial t} \cdot \boldsymbol{\varphi} \,\mathrm{d}x + \int_\Omega \sum_{i=1}^N \frac{\partial \boldsymbol{f}_i(\boldsymbol{w})}{\partial x_i} \cdot \boldsymbol{\varphi} \,\mathrm{d}x \\ &\quad + \int_\Omega \sum_{i=1}^N \boldsymbol{R}_i(\boldsymbol{w}, \nabla \boldsymbol{w}) \cdot \frac{\partial \boldsymbol{\varphi}}{\partial x_i} \,\mathrm{d}x \\ &- \int_{\partial\Omega} \sum_{i=1}^N n_i \boldsymbol{R}_i(\boldsymbol{w}, \nabla \boldsymbol{w}) \cdot \boldsymbol{\varphi} \,\mathrm{d}S = 0. \end{aligned} \tag{3.1.10}$$

From the representation of $\boldsymbol{R}_i$ in (3.1.2), boundary conditions and the definition of the space $\boldsymbol{V}$ we find that

$$\int_{\partial\Omega} \sum_{i=1}^N n_i \boldsymbol{R}_i(\boldsymbol{w}, \nabla \boldsymbol{w}) \cdot \boldsymbol{\varphi} \,\mathrm{d}S = 0. \tag{3.1.11}$$

Let us introduce the notation

$$\begin{aligned} (\boldsymbol{w}, \boldsymbol{\varphi}) &= \int_\Omega \boldsymbol{w} \cdot \boldsymbol{\varphi} \,\mathrm{d}x, \\ a(\boldsymbol{w}, \boldsymbol{\varphi}) &= \int_\Omega \sum_{i=1}^N \boldsymbol{R}_i(\boldsymbol{w}, \nabla \boldsymbol{w}) \cdot \frac{\partial \boldsymbol{\varphi}}{\partial x_i} \,\mathrm{d}x, \\ b(\boldsymbol{w}, \boldsymbol{\varphi}) &= \int_\Omega \sum_{i=1}^N \frac{\partial \boldsymbol{f}_i(\boldsymbol{w})}{\partial x_i} \cdot \boldsymbol{\varphi} \,\mathrm{d}x. \end{aligned} \tag{3.1.12}$$

Obviously, the forms given in (3.1.12). are linear with respect to $\boldsymbol{\varphi}$ and make sense for functions $\boldsymbol{w}$ with weaker regularity than that of the classical solution. We shall not specify it here. From the point of view of the FE solution, it is sufficient to write the *weak formulation* of problem (CFP) as the conditions

$$\begin{aligned} &\text{a)}\ \ \boldsymbol{w}(t) - \boldsymbol{w}^*(t) \in \boldsymbol{V}, \quad t \in (0, T), \\ &\text{b)}\ \ \left(\frac{\partial \boldsymbol{w}(t)}{\partial t}, \boldsymbol{\varphi} \right) + a(\boldsymbol{w}(t), \boldsymbol{\varphi}) + b(\boldsymbol{w}(t), \boldsymbol{\varphi}) = 0, \\ &\qquad \forall \boldsymbol{\varphi} \in \boldsymbol{V},\ t \in (0, T), \\ &\text{c)}\ \ \boldsymbol{w}(0) = \boldsymbol{w}^0. \end{aligned} \tag{3.1.13}$$

(Let us recall that $\boldsymbol{w}(t)$ is such a function that $\boldsymbol{w}(t)(x) = \boldsymbol{w}(x, t)$ for $x \in \Omega$.) A function $\boldsymbol{w}$ for which the individual terms in (3.1.13), b) make sense, satisfying conditions (3.1.13), a)-c) is called a *weak solution* of the compressible flow problem (CFP).

Here $\boldsymbol{w}^* : [0,T] \to H^1(\Omega)^m$ is a function satisfying the Dirichlet boundary conditions (3.1.6), i.e.

$$w_1^* = \rho_D, (w_2^*, \ldots, w_{m-1}^*) = \rho_D \boldsymbol{v}_D, w_m^* = E_D \quad \text{on } \Gamma_I \times (0,T), \tag{3.1.14}$$
$$w_2^* = \ldots = w_{m-1}^* = 0 \quad \text{on } \Gamma_W \times (0,T).$$

3.1.1 *Computational grids*

By Ω_h we denote a polygonal ($N = 2$) or polyhedral ($N = 3$) approximation of the domain Ω. In the combined FV–FE method we work with two meshes constructed in the domain Ω_h: a finite element mesh $\mathcal{T}_h = \{K_i\}_{i \in I}$ and a finite volume mesh $\mathcal{D}_h = \{D_j\}_{j \in J}$. Here, I and $J \subset Z^+$ are suitable index sets.

The FE mesh $\mathcal{T}_h$ satisfies the standard properties from the FEM. It is formed by a finite number of closed triangles ($N = 2$) or tetrahedra ($N = 3$) $K = K_i$ covering the closure of Ω_h,

$$\overline{\Omega}_h = \bigcup_{K \in \mathcal{T}_h} K. \tag{3.1.15}$$

By σ_h we denote the set of all vertices of all elements $K \in \mathcal{T}_h$ and assume that $\sigma_h \cap \partial\Omega_h \subset \partial\Omega$. Moreover, let the common points of sets Γ_I, Γ_W and Γ_O belong to the set σ_h. The symbol $\mathcal{Q}_h$ will denote the set of all midpoints of sides of all elements $K \in \mathcal{T}$. By $|K|$ we denote the N-dimensional measure of $K \in \mathcal{T}_h$ (i.e. $|K|$ is the area of K, if $N = 2$, and $|K|$ is the volume of K, if $N = 3$), $h_K = \operatorname{diam}(K)$ and ρ_K is the radius of the largest ball inscribed in K. We set $h = \max_{K \in \mathcal{T}_h} h_K$.

We shall also work with an FV mesh $\mathcal{D}_h$ in Ω_h, formed by a finite number of closed polygons ($N = 2$) or polyhedra ($N = 3$) such that

$$\overline{\Omega}_h = \bigcup_{D \in \mathcal{D}_h} D. \tag{3.1.16}$$

Various types of FV meshes were introduced in Section 2.1.

We use the same notation as in Section 2.2.1. The boundary ∂D_i of each finite volume $D_i \in \mathcal{D}_h$ can be expressed as

$$\partial D_i = \bigcup_{j \in S(i)} \bigcup_{\alpha=1}^{\beta_{ij}} \Gamma_{ij}^{\alpha}, \tag{3.1.17}$$

where Γ_{ij}^{α} are straight segments ($N = 2$) or plane manifolds ($N = 3$), called faces of D_i, $\Gamma_{ij}^{\alpha} = \Gamma_{ji}^{\alpha}$, which either form the common boundary of neighbouring finite volumes D_i and D_j or are part of $\partial\Omega_h$. We denote by $|D_i|$ the N-dimensional measure of D_i, $|\Gamma_{ij}^{\alpha}|-$ the $(N-1)$-dimensional measure of Γ_{ij}^{α}, $\boldsymbol{n}_{ij}^{\alpha}$ – the unit outer normal to ∂D_i on Γ_{ij}^{α}. Clearly, $\boldsymbol{n}_{ij}^{\alpha} = -\boldsymbol{n}_{ji}^{\alpha}$. $S(i)$ is a suitable index set written in the form

$$S(i) = s(i) \cup \gamma(i), \tag{3.1.18}$$

where $s(i)$ contains indexes of neighbours D_j of D_i and $\gamma(i)$ is formed by indexes j of $\Gamma_{ij}^1 \subset \partial\Omega_h$ (in this case we set $\beta_{ij} = 1$). For details see Section 2.2.1.

3.1.2 *FV and FE spaces*

The FE approximate solution will be sought in a finite dimensional space

$$\boldsymbol{X}_h = X_h^m, \tag{3.1.19}$$

called a *finite element space*. We shall consider two cases of the definition of X_h:

$$X_h = \left\{\varphi_h \in C(\overline{\Omega}_h); \varphi_h|_K \in P^1(K)\ \forall K \in \mathcal{T}_h\right\} \tag{3.1.20}$$

(conforming piecewise linear elements) and

$$X_h = \left\{\varphi_h \in L^2(\Omega); \varphi_h|_K \in P^1(K),\ \varphi_h \text{ are continuous at midpoints } Q_j \in \mathcal{Q} \text{ of all faces of all } K \in \mathcal{T}_h\right\} \tag{3.1.21}$$

(nonconforming Crouzeix–Raviart piecewise linear elements – they were originally proposed for the approximation of the velocity of incompressible flow, see (Crouzeix and Raviart, 1973), (Feistauer, 1993)).

The finite volume approximation is an element of the finite volume space

$$\boldsymbol{Z}_h = Z_h^m, \tag{3.1.22}$$

where

$$Z_h = \left\{\varphi_h \in L^2(\Omega); \varphi_h|_D = \text{const}\ \forall D \in \mathcal{D}_h\right\}. \tag{3.1.23}$$

One of the most important concepts is a relation between the spaces $\boldsymbol{X}_h$ and $\boldsymbol{Z}_h$. We assume the existence of a mapping $L_h : \boldsymbol{X}_h \to \boldsymbol{Z}_h$, called a *lumping operator*.

In practical computations the following combinations of the FV and FE spaces are used (see, for example, (Feistauer and Felcman, 1997), (Feistauer *et al.*, 1995), (Feistauer *et al.*, 1996), (Dolejší *et al.*, 2002)).

a) *Conforming finite elements combined with dual finite volumes* In this case the FE space $\boldsymbol{X}_h$ is defined by (3.1.19) – (3.1.20). The mesh $\mathcal{D}_h$ is formed by dual FVs D_i constructed over the mesh $\mathcal{T}_h$, associated with vertices $P_i \in \sigma_h = \{P_i\}_{i\in J}$. In this case, the lumping operator is defined as such a mapping $L_h : \boldsymbol{X}_h \to \boldsymbol{Z}_h$ that for each $\boldsymbol{\varphi}_h \in \boldsymbol{X}_h$

$$L_h\boldsymbol{\varphi}_h \in \boldsymbol{Z}_h, \quad L_h\boldsymbol{\varphi}_h|_{D_i} = \boldsymbol{\varphi}_h(P_i) \quad \forall i \in J. \tag{3.1.24}$$

Obviously, L_h is a one-to-one mapping of $\boldsymbol{X}_h$ onto $\boldsymbol{Z}_h$.

b) *Nonconforming finite elements combined with barycentric finite volumes* Now let $\mathcal{Q}_h = \{Q_i; i \in J\}$ denote the set of centres of faces of all $K \in \mathcal{T}_h$. Then $\mathcal{D}_h = \{D_i\}_{i\in J}$ is the mesh formed by barycentric FVs constructed over $\mathcal{T}_h$, associated with Q_i, $i \in J$, as described in Sections 2.2.1.1, d) for $N = 2$. The space $\boldsymbol{X}_h$ is given in (3.1.19) and (3.1.21) and L_h is defined by

$$L_h\boldsymbol{\varphi}_h \in \boldsymbol{Z}_h, \quad L_h\varphi_h|_{D_i} = \varphi_h(Q_i), \quad i \in J, \tag{3.1.25}$$

for any $\varphi_h \in \boldsymbol{X}_h$. Again, L_h is a one-to-one mapping of $\boldsymbol{X}_h$ onto $\boldsymbol{Z}_h$.

c) *Combination of conforming triangular finite elements with triangular finite volumes* is another possibility. It gives good results, but theory is still missing. We do not introduce details here.

3.1.3 *Space semidiscretization of the problem*

We use the following approximations: $\Omega \approx \Omega_h$, $\Gamma_I \approx \Gamma_{Ih} \subset \partial\Omega_h$, $\Gamma_W \approx \Gamma_{Wh} \subset \partial\Omega_h$, $\Gamma_O \approx \Gamma_{Oh} \subset \partial\Omega_h$, $\boldsymbol{w}(t) \approx \boldsymbol{w}_h(t) \in \boldsymbol{X}_h$, $\boldsymbol{\varphi} \approx \boldsymbol{\varphi}_h \in \boldsymbol{V}_h \approx \boldsymbol{V}$, where

$$\boldsymbol{V}_h = \Big\{\boldsymbol{\varphi}_h = (\varphi_{h1}, \dots, \varphi_{hm}) \in \boldsymbol{X}_h; \boldsymbol{\varphi}(P_i) = 0 \tag{3.1.26}$$
$$\text{at } P_i \in \Gamma_{Ih}, \varphi_{hn}(P_i) = 0 \text{ for } n = 2, \dots, m-1 \text{ at } P_i \in \Gamma_{Wh}\Big\}.$$

Here P_i denote nodes, i.e. vertices $P_i \in \sigma_h$ or midpoints of faces $P_i \in \mathcal{Q}_h$ in the case of conforming or nonconforming finite elements, respectively.

The form $a(\boldsymbol{w}, \boldsymbol{\varphi})$ defined in (3.1.12) is approximated by

$$\tilde{a}(\boldsymbol{w}_h, \boldsymbol{\varphi}_h) = \sum_{K \in \mathcal{T}_h} \int_K \sum_{s=1}^N \boldsymbol{R}_s(\boldsymbol{w}_h, \nabla \boldsymbol{w}_h) \cdot \frac{\partial \boldsymbol{\varphi}_h}{\partial x_s} \,\mathrm{d}x, \quad \boldsymbol{w}_h, \boldsymbol{\varphi}_h \in \boldsymbol{X}_h. \tag{3.1.27}$$

In order to approximate the nonlinear convective terms containing inviscid fluxes $\boldsymbol{f}_s$, we start from the analogy with the form b from (3.1.12) written as $\int_\Omega \sum_{s=1}^N (\partial \boldsymbol{f}_s(\boldsymbol{w})/\partial x_s) \cdot \boldsymbol{\varphi} \,\mathrm{d}x$, where we use the approximation $\boldsymbol{\varphi} \approx L_h \boldsymbol{\varphi}_h$. Then Green's theorem is applied and the flux $\sum_{s=1}^N f_s(\boldsymbol{w}) n_s$ is approximated with the aid of a numerical flux $\boldsymbol{H}(\boldsymbol{w}, \boldsymbol{w}', \boldsymbol{n})$ from the FVM treated in Section 2.1:

$$\begin{aligned}
&\int_\Omega \sum_{s=1}^N \frac{\partial \boldsymbol{f}_s(\boldsymbol{w})}{\partial x_s} \cdot \boldsymbol{\varphi} \mathrm{d}x \approx \sum_{i \in J} \int_{D_i} \sum_{s=1}^N \frac{\partial \boldsymbol{f}_s(\boldsymbol{w})}{\partial x_s} \cdot L_h \boldsymbol{\varphi}_h \,\mathrm{d}x \\
&= \sum_{i \in J} L_h \boldsymbol{\varphi}_h|_{D_i} \cdot \int_{D_i} \sum_{s=1}^N \frac{\partial \boldsymbol{f}_s(\boldsymbol{w})}{\partial x_s} \,\mathrm{d}x \\
&= \sum_{i \in J} L_h \boldsymbol{\varphi}_h|_{D_i} \cdot \int_{\partial D_i} \sum_{s=1}^N \boldsymbol{f}_s(\boldsymbol{w}) n_s \,\mathrm{d}S \\
&= \sum_{i \in J} L_h \boldsymbol{\varphi}_h|_{D_i} \cdot \sum_{j \in S(i)} \sum_{\alpha=1}^{\beta_{ij}} \int_{\Gamma_{ij}^\alpha} \sum_{s=1}^N \boldsymbol{f}_s(\boldsymbol{w}) n_s \,\mathrm{d}S \\
&\approx \sum_{i \in J} L_h \boldsymbol{\varphi}_h|_{D_i} \cdot \sum_{j \in S(i)} \sum_{\alpha=1}^{\beta_{ij}} \boldsymbol{H}(L_h \boldsymbol{w}_h|_{D_i}, L_h \boldsymbol{w}_h|D_j, \boldsymbol{n}_{ij}^\alpha)|\Gamma_{ij}^\alpha|.
\end{aligned} \tag{3.1.28}$$

Hence, we set

$$b_h(\boldsymbol{w}_h, \boldsymbol{\varphi}_h) = \sum_{i \in J} L_h \boldsymbol{\varphi}_h|_{D_i} \cdot \sum_{j \in S(i)} \sum_{\alpha=1}^{\beta_{ij}} \boldsymbol{H}(L_h \boldsymbol{w}_h|_{D_i}, L_h \boldsymbol{w}_h|_{D_j}, \boldsymbol{n}_{ij}^\alpha)|\Gamma_{ij}^\alpha|. \tag{3.1.29}$$

If $\Gamma_{ij}^\alpha \subset \partial\Omega_h$, it is necessary to give an interpretation of $L_h w_h|_{D_j}$ using inviscid boundary conditions – see Section 3.1.5.

In practical computations, the integrals are evaluated approximately with the aid of numerical quadratures. Then the $L^2(\Omega)$-scalar product is approximated by the form $(\boldsymbol{w}_h, \boldsymbol{\varphi}_h)_h$ and the form a_h approximates $\tilde{a}_h$.

Definition 3.1 *We define a finite volume–finite element approximate solution of the viscous compressible flow as a vector-valued function $\boldsymbol{w}_h = \boldsymbol{w}_h(x,t)$ defined for (a.a) $x \in \overline{\Omega}_h$ and all $t \in [0,T]$ satisfying the following conditions:*

$$
\begin{aligned}
&a)\ \ \boldsymbol{w}_h \in C^1([0,T]; \boldsymbol{X}_h), \\
&b)\ \ \boldsymbol{w}_h(t) - \boldsymbol{w}_h^*(t) \in \boldsymbol{V}_h, \\
&c)\ \ \left(\frac{\partial \boldsymbol{w}_h(t)}{\partial t}, \boldsymbol{\varphi}_h\right)_h + b_h(\boldsymbol{w}_h(t), \boldsymbol{\varphi}_h) \\
&\qquad + a_h(\boldsymbol{w}_h(t), \boldsymbol{\varphi}_h) = 0 \\
&\qquad \forall \boldsymbol{\varphi}_h \in \boldsymbol{V}_h,\ \forall t \in (0,T), \\
&d)\ \ \boldsymbol{w}_h(0) = \boldsymbol{w}_h^0.
\end{aligned}
\tag{3.1.30}
$$

3.1.4 *Time discretization*

Problem (3.1.30) is equivalent to a large system of ordinary differential equations which is solved with the aid of a suitable time discretization. It is possible to use Runge–Kutta methods.

The simpliest possibility is the *Euler forward scheme*. Let $0 = t_0 < t_1 < t_2 \ldots$ be a partition of the time interval and let $\tau_k = t_{k+1} - t_k$. Then in (3.1.30), b), c) we use the approximations $\boldsymbol{w}_h^k \approx \boldsymbol{w}_h(t_k)$ and $(\partial \boldsymbol{w}_h/\partial t)(t_k) \approx (\boldsymbol{w}_h^{k+1} - \boldsymbol{w}_h^k)/\tau_k$ and obtain the scheme

$$
\begin{aligned}
&\text{a)}\ \ \boldsymbol{w}_h^{k+1} - \boldsymbol{w}_h^*(t_{k+1}) \in \boldsymbol{V}_h, \\
&\text{b)}\ \ (\boldsymbol{w}_h^{k+1}, \boldsymbol{\varphi}_h)_h = (\boldsymbol{w}_h^k, \boldsymbol{\varphi}_h)_h - \tau_k a_h(\boldsymbol{w}_h^k, \boldsymbol{\varphi}_h) \\
&\qquad - \tau_k b_k(\boldsymbol{w}_h^k, \boldsymbol{\varphi}_h) \quad \forall \boldsymbol{\varphi}_h \in \boldsymbol{V}_h,\ k = 0, 1, \ldots.
\end{aligned}
\tag{3.1.31}
$$

3.1.5 *Realization of boundary conditions in the convective form b_h*

If $\Gamma_{ij}^\alpha \subset \partial\Omega_h$ (i.e. $j \in \gamma(i),\ \alpha = 1$), then there is no finite volume adjacent to Γ_{ij}^α from the opposite side to D_i and it is necessary to interpret the value $L_h \boldsymbol{w}_h^k|_{D_j}$ in the definition (3.1.29) of the form b_h. This means that we need to determine a boundary state $\tilde{\boldsymbol{w}}_j^k$ which will be substituted for $L_h \boldsymbol{w}_h^k|_{D_j}$ in (3.1.29).

We apply the approach used in the FVM and explained in Section 2.2.5. This means that the individual components of the state vector $\tilde{\boldsymbol{w}}_j^k$ are either extrapolated (with the use of $L_h \boldsymbol{w}_h^k|_{D_i}$) or prescribed, according to the signs of eigenvalues of the matrix $\mathbb{P}(\boldsymbol{w}_h^k|_{D_i}, \boldsymbol{n}_{ij}^\alpha)$ – cf. 2.2.5. For example, in the case of the *subsonic outlet*, the auxiliary outlet pressure p_D is prescribed on Γ_O.

3.1.5.1 *Stability of the combined FV–FE methods* Since scheme (3.1.31) is explicit, it is necessary to apply some stability condition. Unfortunately, there is no rigorous theory for the stability of schemes applied to the complete compressible Navier–Stokes system. We proceed heuristically. By virtue of the explicit

FV discretization of inviscid terms, we apply the modification of the stability condition derived in Section 2.2.8 for the explicit FVM for the solution of the Euler equations:

$$\frac{\tau_k}{|D_i|} \max_{\substack{j\in S(i)\\ \alpha=1,\dots,\beta_{ij}}} \max_{\ell=1,\dots,m} \{|\partial D_i||\lambda_\ell(\boldsymbol{w}_i^k, \boldsymbol{n}_{ij}^\alpha)| + \mu\} \le \mathrm{CFL} \approx 0.85, \quad i \in J, \quad (3.1.32)$$

where $\lambda_\ell(\boldsymbol{w}_i^k, \boldsymbol{n}_{ij}^\alpha)$ are the eigenvalues of the matrix $\mathbb{P}(\boldsymbol{w}_i^k, \boldsymbol{n}_{ij}^\alpha)$ – see (2.1.7).

In the case of the implicit discretization of the viscous terms we omit μ in the above CFL condition.

3.2 Discontinuous Galerkin finite element method

This section is concerned with the discontinuous Galerkin finite element method (DGFEM) for the numerical solution of compressible inviscid as well as viscous flow. The DGFEM is based on the use of piecewise polynomial approximations without any requirement on the continuity on interfaces between neighbouring elements. It uses advantages of the FVM and FEM.

3.2.1 *DGFEM for conservation laws*

In this section we shall discuss the discontinuous Galerkin finite element discretization of multidimensional initial-boundary value problems for conservation law equations and, in particular, for the Euler equations. Let $\Omega \subset \mathbb{R}^N$ be a bounded domain with a piecewise smooth Lipschitz-continuous boundary $\partial\Omega$ and let $T > 0$. In the space-time cylinder $Q_T = \Omega \times (0, T)$ we consider a system of m first order hyperbolic equations

$$\frac{\partial \boldsymbol{w}}{\partial t} + \sum_{s=1}^{N} \frac{\partial \boldsymbol{f}_s(\boldsymbol{w})}{\partial x_s} = 0. \quad (3.2.1)$$

This system is equipped with the initial condition

$$\boldsymbol{w}(x, 0) = \boldsymbol{w}^0(x), \quad x \in \Omega, \quad (3.2.2)$$

where $\boldsymbol{w}^0$ is a given function, and with boundary conditions

$$B(\boldsymbol{w}) = 0, \quad (3.2.3)$$

where B is a boundary operator. The choice of the boundary conditions is carried out similarly as in Section 2.2.5 in the framework of the discrete problem for the Euler equations describing gas flow.

3.2.1.1 *Discretization* Let Ω be a polygonal or polyhedral domain, if $N = 2$ or $N = 3$, respectively. Let $\mathcal{T}_h$ $(h > 0)$ denote a partition of the closure $\overline{\Omega}$ of the domain Ω into a finite number of closed convex polygons (if $N = 2$) or polyhedra (if $N = 3$) K with mutually disjoint interiors. We call $\mathcal{T}_h$ a triangulation of Ω, but *do not* require the usual conforming properties from the FEM. In 2D problems

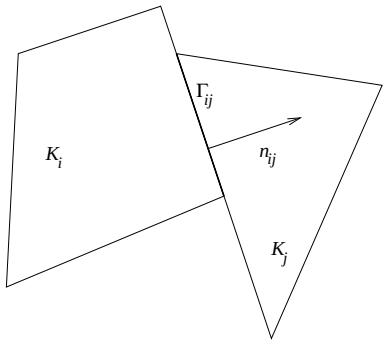

FIG. 3.1. Neighbouring elements $K_i,\ K_j$

we usually choose $K \in \mathcal{T}_h$ as triangles or quadrilaterals, in 3D, $K \in \mathcal{T}_h$ can be, for example, tetrahedra, pyramids or hexahedra, but we can allow even more general convex elements K.

We set $h_K = \mathrm{diam}(K)$, $h = \max_{K\in\mathcal{T}_h} h_K$. By $|K|$ we denote the N-dimensional Lebesgue measure of K. All elements of $\mathcal{T}_h$ will be numbered so that $\mathcal{T}_h = \{K_i\}_{i\in I}$, where $I \subset Z^+ = \{0, 1, 2, \ldots\}$ is a suitable index set. If two elements $K_i,\ K_j \in \mathcal{T}_h$ contain a nonempty open face which is a part of an $(N-1)$-dimensional hyperplane (i.e. straight line in 2D or plane in 3D), we call them *neighbouring elements* or *neighbours*. In this case we set $\Gamma_{ij} = \partial K_i \cap \partial K_j$ and assume that the whole set Γ_{ij} is a part of an $(N-1)$-dimensional hyperplane. For $i \in I$ we set $s(i) = \{j \in I; K_j \text{ is a neighbour of } K_i\}$. The boundary $\partial\Omega$ is formed by a finite number of faces of elements K_i adjacent to $\partial\Omega$. We denote all these boundary faces by S_j, where $j \in I_b \subset Z^- = \{-1, -2, \ldots\}$, and set $\gamma(i) = \{j \in I_b; S_j \text{ is a face of } K_i\}, \Gamma_{ij} = S_j$ for $K_i \in \mathcal{T}_h$ such that $S_j \subset \partial K_i,\ j \in I_b$. For K_i not containing any boundary face S_j we set $\gamma(i) = \emptyset$. Obviously, $s(i) \cap \gamma(i) = \emptyset$ for all $i \in I$. Now, if we write $S(i) = s(i) \cup \gamma(i)$, we have

$$\partial K_i = \bigcup_{j\in S(i)} \Gamma_{ij}, \qquad \partial K_i \cap \partial\Omega = \bigcup_{j\in\gamma(i)} \Gamma_{ij}. \tag{3.2.4}$$

Furthermore, we use the following notation: $\boldsymbol{n}_{ij} = ((n_{ij})_1, \ldots, (n_{ij})_N)$ is the unit outer normal to ∂K_i on the face Γ_{ij} ($\boldsymbol{n}_{ij}$ is a constant vector on Γ_{ij}), $d(\Gamma_{ij}) = \mathrm{diam}(\Gamma_{ij})$, and $|\Gamma_{ij}|$ is the $(N-1)$-dimensional Lebesgue measure of Γ_{ij}. See Fig. 3.1.

Over the triangulation $\mathcal{T}_h$ we define the *broken Sobolev space*

$$H^k(\Omega, \mathcal{T}_h) = \{v; v|_K \in H^k(K)\ \forall K \in \mathcal{T}_h\}. \tag{3.2.5}$$

For $v \in H^1(\Omega, \mathcal{T}_h)$ we introduce the following notation:

$$v|_{\Gamma_{ij}} - \text{the trace of} \quad v|_{K_i} \quad \text{on} \quad \Gamma_{ij}, \tag{3.2.6}$$

$$v|_{\Gamma_{ji}} - \text{the trace of} \quad v|_{K_j} \quad \text{on} \quad \Gamma_{ji} = \Gamma_{ij}.$$

The approximate solution of problem (3.2.1)–(3.2.3) is sought in the space of discontinuous piecewise polynomial vector-valued functions $\boldsymbol{S}_h$ defined by

$$\begin{aligned} &\boldsymbol{S}_h = [S_h]^m, \\ &S_h = S^{r,-1}(\Omega, \mathcal{T}_h) = \{v; v|_K \in P^r(K)\ \forall\, K \in \mathcal{T}_h\}, \end{aligned} \tag{3.2.7}$$

where $r \in Z^+$ and $P^r(K)$ denotes the space of all polynomials on K of degree $\leq r$.

Let us assume that $\boldsymbol{w}$ is a classical C^1-solution of system (3.2.1). As usual, by $\boldsymbol{w}(t)$ we denote a function $\boldsymbol{w}(t) : \Omega \to I\!R^m$ such that $\boldsymbol{w}(t)(x) = \boldsymbol{w}(x,t)$ for $x \in \Omega$. In order to derive the discrete problem, we multiply (3.2.1) by a function $\boldsymbol{\varphi} \in H^1(\Omega, \mathcal{T}_h)^m$ and integrate over an element $K_i,\ i \in I$. With the use of Green's theorem, we obtain the integral identity

$$\begin{aligned} \frac{\mathrm{d}}{\mathrm{d}t} \int_{K_i} \boldsymbol{w}(t) \cdot \boldsymbol{\varphi}\, \mathrm{d}x - \int_{K_i} \sum_{s=1}^{N} \boldsymbol{f}_s(\boldsymbol{w}(t)) \cdot \frac{\partial \boldsymbol{\varphi}}{\partial x_s}\, \mathrm{d}x \\ + \sum_{j \in S(i)} \int_{\Gamma_{ij}} \sum_{s=1}^{N} \boldsymbol{f}_s(\boldsymbol{w}(t)) \cdot \boldsymbol{\varphi}\, n_s\, \mathrm{d}S = 0. \end{aligned} \tag{3.2.8}$$

Summing (3.2.8) over all $K_i \in \mathcal{T}_h$, we obtain the identity

$$\begin{aligned} \frac{\mathrm{d}}{\mathrm{d}t} \sum_{i \in I} \int_{K_i} \boldsymbol{w}(t) \cdot \boldsymbol{\varphi}\, \mathrm{d}x - \sum_{i \in I} \int_{K_i} \sum_{s=1}^{N} \boldsymbol{f}_s(\boldsymbol{w}(t)) \cdot \frac{\partial \boldsymbol{\varphi}}{\partial x_s}\, \mathrm{d}x \\ + \sum_{i \in I} \sum_{j \in S(i)} \int_{\Gamma_{ij}} \sum_{s=1}^{N} \boldsymbol{f}_s(\boldsymbol{w}(t)) \cdot \boldsymbol{\varphi}\, n_s\, \mathrm{d}S = 0. \end{aligned} \tag{3.2.9}$$

Under the notation

$$(\boldsymbol{w}, \boldsymbol{\varphi}) = \sum_{i \in I} \int_{K_i} \boldsymbol{w} \cdot \boldsymbol{\varphi}\, \mathrm{d}x = \int_{\Omega} \boldsymbol{w} \cdot \boldsymbol{\varphi} \mathrm{d}x \tag{3.2.10}$$

($[L^2]^m$-scalar product) and

$$\begin{aligned} b(\boldsymbol{w}, \boldsymbol{\varphi}) = -\sum_{i \in I} \int_{K_i} \sum_{s=1}^{N} \boldsymbol{f}_s(\boldsymbol{w}) \cdot \frac{\partial \boldsymbol{\varphi}}{\partial x_s}\, \mathrm{d}x \\ + \sum_{i \in I} \sum_{j \in S(i)} \int_{\Gamma_{ij}} \sum_{s=1}^{N} \boldsymbol{f}_s(\boldsymbol{w}) \cdot \boldsymbol{\varphi}\, n_s\, \mathrm{d}S, \end{aligned} \tag{3.2.11}$$

(3.2.8) can be written in the form

$$\frac{\mathrm{d}}{\mathrm{d}t}(\boldsymbol{w}(t),\boldsymbol{\varphi})+b(\boldsymbol{w}(t),\boldsymbol{\varphi})=0. \tag{3.2.12}$$

This equality represents a *weak form* of system (3.2.1) in the sense of the broken Sobolev space $H^1(\Omega,\mathcal{T}_h)$.

3.2.1.2 *Numerical solution* Now we shall introduce the discrete problem approximating identity (3.2.12). For $t\in[0,T]$, the exact solution $\boldsymbol{w}(t)$ will be approximated by an element $\boldsymbol{w}_h(t)\in\boldsymbol{S}_h$. It is not possible to replace $\boldsymbol{w}$ formally in the definition (3.2.11) of the form b, because $\boldsymbol{w}_h$ is discontinuous on Γ_{ij} in general. Similarly as in the FVM we use here the concept of the *numerical flux* $\boldsymbol{H}=\boldsymbol{H}(\boldsymbol{u},\boldsymbol{v},\boldsymbol{n})$ and write

$$\int_{\Gamma_{ij}}\sum_{s=1}^{N}\boldsymbol{f}_s(\boldsymbol{w}(t))\,n_s\cdot\boldsymbol{\varphi}\,\mathrm{d}S\approx\int_{\Gamma_{ij}}\boldsymbol{H}(\boldsymbol{w}_h|_{\Gamma_{ij}}(t),\boldsymbol{w}_h|_{\Gamma_{ji}}(t),\boldsymbol{n}_{ij})\cdot\boldsymbol{\varphi}|_{\Gamma ij}\,\mathrm{d}S. \tag{3.2.13}$$

We assume that the numerical flux has the properties formulated in Section 2.2.3:

1) $\boldsymbol{H}(\boldsymbol{u},\boldsymbol{v},\boldsymbol{n})$ is defined and continuous on $D\times D\times\mathcal{S}_1$, where D is the domain of definition of the fluxes $\boldsymbol{f}_s$ and $\mathcal{S}_1$ is the unit sphere in $\mathbb{R}^N$: $\mathcal{S}_1=\{\boldsymbol{n}\in\mathbb{R}^N;|\boldsymbol{n}|=1\}$.
2) $\boldsymbol{H}$ is *consistent*:

$$\boldsymbol{H}(\boldsymbol{u},\boldsymbol{u},\boldsymbol{n})=\mathcal{P}(\boldsymbol{u},\boldsymbol{n})=\sum_{s=1}^{N}\boldsymbol{f}_s(\boldsymbol{u})\,n_s,\quad \boldsymbol{u}\in D,\ \boldsymbol{n}\in\mathcal{S}_1. \tag{3.2.14}$$

3) $\boldsymbol{H}$ is *conservative*:

$$\boldsymbol{H}(\boldsymbol{u},\boldsymbol{v},\boldsymbol{n})=-\boldsymbol{H}(\boldsymbol{v},\boldsymbol{u},-\boldsymbol{n}),\quad \boldsymbol{u},\,\boldsymbol{v}\in D,\ \boldsymbol{n}\in\mathcal{S}_1. \tag{3.2.15}$$

The above considerations lead us to the definition of the approximation b_h of the convective form b:

$$\begin{aligned}b_h(\boldsymbol{w},\boldsymbol{\varphi})=&-\sum_{i\in I}\int_{K_i}\sum_{s=1}^{N}\boldsymbol{f}_s(\boldsymbol{w})\cdot\frac{\partial\boldsymbol{\varphi}}{\partial x_s}\,\mathrm{d}x \\ &+\sum_{i\in I}\sum_{j\in S(i)}\int_{\Gamma_{ij}}\boldsymbol{H}(\boldsymbol{w}|_{\Gamma_{ij}},\boldsymbol{w}|_{\Gamma_{ji}},\boldsymbol{n}_{ij})\cdot\boldsymbol{\varphi}|_{\Gamma_{ij}}\mathrm{d}S,\quad \boldsymbol{w},\boldsymbol{\varphi}\in H^1(\Omega,\mathcal{T}_h)^m.\end{aligned} \tag{3.2.16}$$

By $\boldsymbol{w}_h^0$ we denote an $\boldsymbol{S}_h$-approximation of $\boldsymbol{w}^0$, e.g. the $[L^2]^m$-projection on $\boldsymbol{S}_h$.

Now we come to the formulation of the *discrete problem.*

Definition 3.2 *We say that $\boldsymbol{w}_h$ is an approximate solution of* (3.2.12)*, if it satisfies the conditions*

$$a)\ \ \boldsymbol{w}_h\in C^1([0,T];\boldsymbol{S}_h), \tag{3.2.17}$$

$$b)\ \ \frac{\mathrm{d}}{\mathrm{d}t}(\boldsymbol{w}_h(t),\boldsymbol{\varphi}_h)+b_h(\boldsymbol{w}_h(t),\boldsymbol{\varphi}_h)=0\quad\forall\,\boldsymbol{\varphi}_h\in\boldsymbol{S}_h,\forall\,t\in(0,T),$$
$$c)\ \ \boldsymbol{w}_h(0)=\boldsymbol{w}_h^0.$$

The discrete problem (3.2.17) is equivalent to an initial value problem for a system of ordinary differential equations which can be solved by a suitable time stepping numerical method.

Remark 3.3 If we set $r=0$ in the DGFEM for the solution of problem (3.2.1)–(3.2.3), which means that we use a piecewise constant approximation of the solution, then we get the finite volume method described in Section 2.1, where we use the notation $\mathcal{D}_h=\mathcal{T}_h$, $D_i=K_i$ and $J=I, J_b=I_b$. A comparison of the FVM and DGFEM is discussed in (Feistauer, 2002).

3.2.1.3 *Treatment of boundary conditions* If $\Gamma_{ij}\subset\partial\Omega_h$, then there is no neighbour K_j of K_i adjacent to Γ_{ij} and the values of $\boldsymbol{w}|_{\Gamma_{ij}}$ must be determined on the basis of *boundary conditions*. We use the same approach as in the FVM, explained in Section 2.2.5.

3.2.2 *Limiting of the order of accuracy*

Let us return to the discrete problem (3.2.17), equivalent to a system of ordinary differential equations. The simplest way to obtain a fully discrete problem is to use the *Euler forward method*. To this end, we consider a partition $0=t_0<t_1<t_2<\ldots$ of the time interval $(0,T)$ and set $\tau_k=t_{k+1}-t_k$.

Using the approximations $\boldsymbol{w}_h^k\approx\boldsymbol{w}_h(t_k)$, $\frac{\mathrm{d}}{\mathrm{d}t}(\boldsymbol{w}_h(t),\boldsymbol{\varphi}_h)\approx(\boldsymbol{w}_h^{k+1}-\boldsymbol{w}_h^k,\boldsymbol{\varphi}_h)/\tau_k$, we obtain the *fully discrete problem*: for each $k\ge0$ find $\boldsymbol{w}_h^{k+1}$ such that

$$\begin{aligned}&\text{a)}\ \ \boldsymbol{w}_h^{k+1}\in\boldsymbol{S}_h,\\ &\text{b)}\ \ (\boldsymbol{w}_h^{k+1},\boldsymbol{\varphi}_h)=(\boldsymbol{w}_h^k,\boldsymbol{\varphi}_h)-\tau_k b_h(\boldsymbol{w}_h^k,\boldsymbol{\varphi}_h)\quad\forall\,\boldsymbol{\varphi}_h\in\boldsymbol{S}_h.\end{aligned}\tag{3.2.18}$$

More precise time discretization is obtained with the aid of the Runge–Kutta methods.

The disadvantage of higher order schemes is the rise of the Gibbs phenomenon manifested by nonphysical spurious oscillations, undershoots and overshoots in the approximate solution in the vicinity of discontinuities or steep gradients. In order to avoid the Gibbs phenomenon, it is necessary to use a suitable limiting of order of accuracy of the method in a vicinity of discontinuities.

Here we present a limiting proposed in (Dolejší *et al.*, 2003). We explain this approach for a 2D situation.

Let us consider a fully discrete problem (3.2.18) with $N=2$, $\Omega\subset\mathbb{R}^2$, for problem (3.2.1)–(3.2.3) discretized by piecewise linear elements (i.e. $p=1$). The use of the Euler forward time discretization (3.2.18) yields the formal accuracy of order $O(\tau+h^2)$, but the poor time approximation can be 'overkilled' by the choice $\tau=O(h^2)$. We assume, of course, that $h\to0+$ and, thus, $0<h<1$.

Let us denote by u_h^k some scalar quantity characterizing the approximate solution $\boldsymbol{w}_h^k$. (For example, for the Euler equations we choose this quantity as

the density ρ.) By $[u_h^k]_{\Gamma_{ij}}$ we denote the jump of u_h^k on Γ_{ij}, i.e. $[u_h^k]_{\Gamma_{ij}} = u_h^k|_{\Gamma_{ij}} - u_h^k|_{\Gamma_{ji}}$. Further, we define $[u_h^k]_{\partial K_i}$ as a function on ∂K_i such that $[u_h^k]_{\partial K_i}(x) = [u_h^k]_{\Gamma_{ij}}(x)$ for $x \in \partial K_i \cap \Gamma_{ij}$. Numerical experiments show that the interelement jumps in the approximate solution are of the order $O(1)$ on discontinuities, but $O(h^2)$ in the regions where the solution is regular. This leads us to the idea to measure the magnitude of interelement jumps in the integral form by

$$\int_{\partial K_i} [u_h^k]^2 \,\mathrm{d}S, \quad K_i \in \mathcal{T}_h. \tag{3.2.19}$$

We define the *discontinuity indicator*

$$g(i) = \int_{\partial K_i} [u_h^k]^2 \,\mathrm{d}S/h^\alpha, \quad K_i \in \mathcal{T}_h, \tag{3.2.20}$$

where $\alpha \in (1, 5)$, e.g. $\alpha = 5/2$, and introduce the following *adaptive strategy* for an *automatic limiting* of the order of accuracy of scheme (3.2.18):

$$\begin{aligned} &\text{a)}\ \ \boldsymbol{w}_h^{k+1} \in \boldsymbol{S}_h = \boldsymbol{S}_h^{1,-1}(\Omega, \mathcal{T}_h), \\ &\text{b)}\ \ (\boldsymbol{w}_h^{k+1}, \boldsymbol{\varphi}) = (\tilde{\boldsymbol{w}}_h^k, \boldsymbol{\varphi}_h) - \tau_k\, b_h(\tilde{\boldsymbol{w}}_h^k, \boldsymbol{\varphi}_h) \quad \forall\, \boldsymbol{\varphi}_h \in \boldsymbol{S}_h, \end{aligned} \tag{3.2.21}$$

where $\tilde{\boldsymbol{w}}_h^k$ is the modification of $\boldsymbol{w}_h^k$ defined with the aid of our limiting strategy in the following way:

$$\begin{aligned} &\text{a)}\ \ \text{Set } \tilde{\boldsymbol{w}}_h^k|_{K_i} := \boldsymbol{w}_h^k|_{K_i}, \quad \forall\, i \in I. \\ &\text{b)}\ \ \text{If } g(i) > 1 \text{ for some } i \in I, \text{ then } \tilde{\boldsymbol{w}}_h^k|_{K_i} := \pi_0 \boldsymbol{w}_h^k|_{K_i}, \end{aligned} \tag{3.2.22}$$

where

$$\pi_0 \boldsymbol{w}_h^k|_{K_i} = \int_{K_i} \boldsymbol{w}_h^k \,\mathrm{d}x/|K_i|, \quad i \in I. \tag{3.2.23}$$

The described procedure means that in (3.2.22) the limiting of the order of the scheme is applied on elements lying on the discontinuity or in the area with a very steep gradient via the piecewise constant approximation of the numerical solution just on the chosen elements. In other areas, where the solution is regular, the numerical scheme is unchanged and the higher order of accuracy is preserved. (The extension to the case $N = 3$ is straightforward.)

The above approach to the *adaptive limiting* was developed in (Dolejší *et al.*, 2003) and (Dolejší *et al.*, 2002*b*). In (Dolejší *et al.*, 2002*b*), a detailed numerical investigation and verification of this algorithm was carried out. A theoretical justification is still missing.

Example 3.4 In order to demonstrate the applicability of the described limiting procedure, let us consider the scalar 2D Burgers equation

$$\frac{\partial u}{\partial t} + u\,\frac{\partial u}{\partial x_1} + u\,\frac{\partial u}{\partial x_2} = 0 \quad \text{in } \Omega \times (0, T), \tag{3.2.24}$$

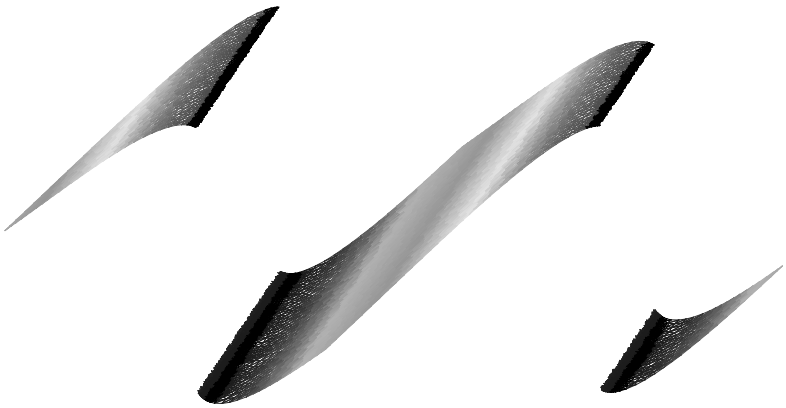

FIG. 3.2. Exact solution of the problem from Example 3.4 plotted at $t = 0.45$

where $\Omega = (-1, 1) \times (-1, 1)$, equipped with initial condition

$$u^0(x_1, x_1) = 0.25 + 0.5 \sin(\pi(x_1 + x_2)), \quad (x_1, x_2) \in \Omega, \tag{3.2.25}$$

and periodic boundary conditions. The exact entropy solution of this problem becomes discontinuous for $t \geq 0.3$ In Fig. 3.2, the graph of the exact solution at time $t = 0.45$ is plotted. If we apply scheme (3.2.18) to this problem on the mesh from Fig. 3.3, with time step $\tau = 2.5 \cdot 10^{-4}$, we obtain the numerical solution shown in Fig. 3.4. It can be seen here that the numerical solution contains spurious overshoots and undershoots near discontinuities. The application of the described limiting procedure avoids them, as shown in Fig. 3.5. In our numerical experiments we use the numerical flux of the form

$$H(u_1, u_2, \boldsymbol{n}) = \begin{cases} \sum_{s=1}^{2} f_s(u_1)\, n_s, \text{ if } A > 0, \\ \sum_{s=1}^{2} f_s(u_2)\, n_s, \text{ if } A \leq 0, \end{cases} \tag{3.2.26}$$

where $f_s(u) = u^2/2$, $A = \sum_{s=1}^{2} f_s'((u_1 + u_2)/2)\, n_s$.

3.2.3 *Approximation of the boundary*

In the FVM applied to conservation laws or in the FEM using piecewise linear approximations applied to elliptic or parabolic problems, it is sufficient to use a polygonal or polyhedral approximation Ω_h of the 2D or 3D domain Ω, respectively. However, numerical experiments show that in some cases the DGFEM does not give a good resolution in the neighbourhood of curved parts of the boundary $\partial\Omega$, if the mentioned approximations of Ω are used. In 1997, Bassi and Rebay (Bassi and Rebay, 1997*b*) showed the importance of a sufficiently accurate approximation of the boundary $\partial\Omega$. For example, if a polygonal approximation of a plane domain is used in the case of flow past a cylinder, then each of the

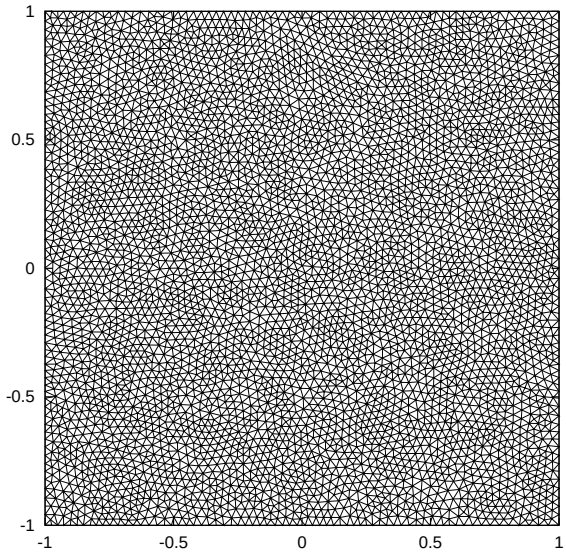

FIG. 3.3. Triangulation used for the numerical solution

vertices of the polygon introduces nonphysical entropy production and the approximate solution presents a nonphysical wake which does not disappear by further refining the grid.

In order to get a good quality numerical solution, it is necessary to use a sufficiently precise approximation of the boundary. For example, if we use piecewise linear elements, then one must use a bilinear transformation of a reference element on a curved boundary element, see Fig. 3.6 and Fig. 3.7.

Then triangles $K_i,\ i \in I_c$, are replaced by the curved triangles and integrals are evaluated on the reference triangle with the aid of a substitution theorem.

3.2.4 *DGFEM for convection–diffusion problems and viscous flow*

3.2.4.1 *Example of a scalar problem* First let us consider a simple scalar nonstationary nonlinear convection-diffusion problem to find $u : Q_T = \Omega \times (0,T) \to \mathbb{R}$ such that

$$\text{a)}\ \ \frac{\partial u}{\partial t} + \sum_{s=1}^{N} \frac{\partial f_s(u)}{\partial x_s} = \nu \Delta u + g \quad \text{in } Q_T, \tag{3.2.27}$$

$$\text{b)}\ \ u\big|_{\Gamma_D \times (0,T)} = u_D, \quad \text{c)}\ \ \nu \frac{\partial u}{\partial n}\Big|_{\Gamma_N \times (0,T)} = g_N,$$

$$\text{d)}\ \ u(x,0) = u^0(x), \quad x \in \Omega.$$

We assume that $\Omega \subset \mathbb{R}^N$ is a bounded polygonal domain, if $N = 2$, or polyhedral domain, if $N = 3$, with a Lipschitz boundary $\partial\Omega = \overline{\Gamma}_D \cup \overline{\Gamma}_N$, $\Gamma_D \cap \Gamma_N = \emptyset$,

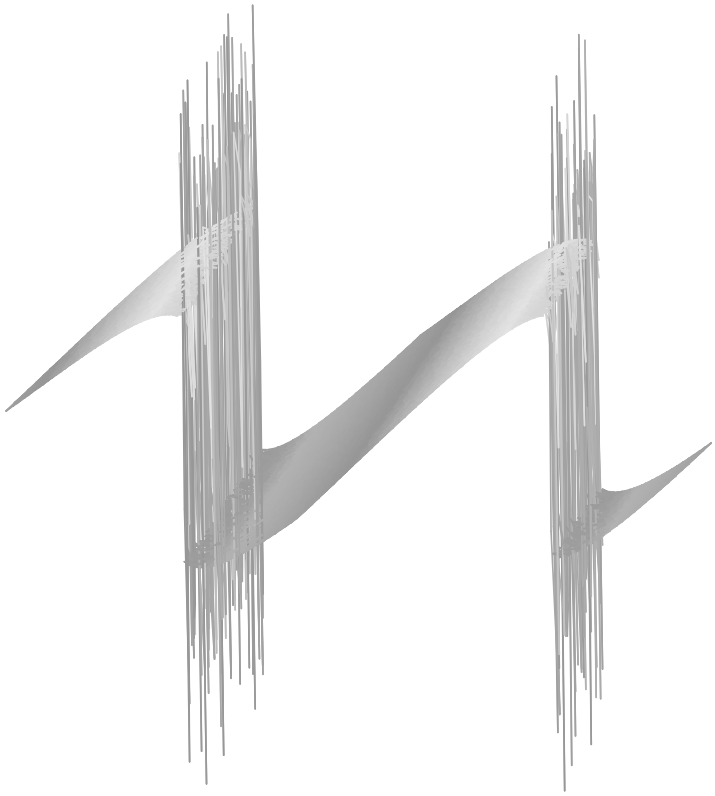

FIG. 3.4. Numerical solution of the problem from Example 3.4 computed by DGFEM, plotted at $t = 0.45$

and $T > 0$. The diffusion coefficient $\nu > 0$ is a given constant, $g : Q_T \to \mathbb{R}$, $u_D : \Gamma_D \times (0,T) \to \mathbb{R}$, $g_N : \Gamma_N \times (0,T) \to \mathbb{R}$ and $u^0 : \Omega \to \mathbb{R}$ are given functions, $f_s \in C^1(\mathbb{R})$, $s = 1, \ldots, N$, are given inviscid fluxes.

We define a *classical solution* of problem (3.2.27) as a sufficiently regular function in $\overline{Q}_T$ satisfying (3.2.27), a)–d) pointwise.

We leave to the reader the definition of a weak solution to problem (3.2.27) as an exercise.

3.2.4.2 *Discretization* The discretization of convective terms is carried out in the same way as in Section 3.2.1.1. There are several approaches to the discretization of the diffusion term. For example, in (Cockburn, 1999) the so-called *local discontinuous Galerkin FEM* is described. It is based on a mixed formulation introducing first-order derivatives of unknown functions as new dependent variables. This method is also used in (Karniadakis and Sherwin, 1999) in spectral methods and in (Bassi and Rebay, 1997*a*). Its theoretical analysis can be

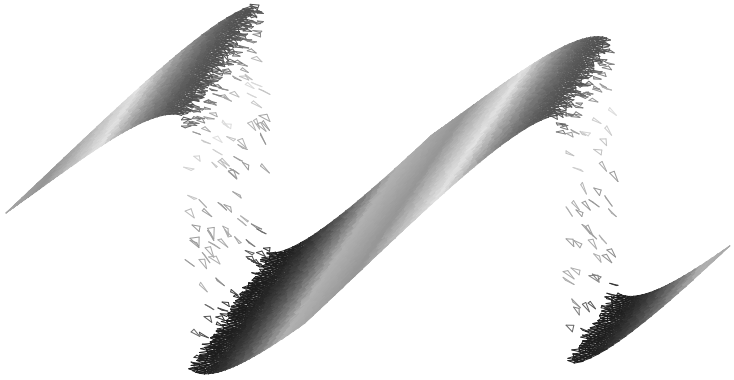

FIG. 3.5. Numerical solution of the problem from Example 3.4 computed by DGFEM with limiting, plotted at $t = 0.45$

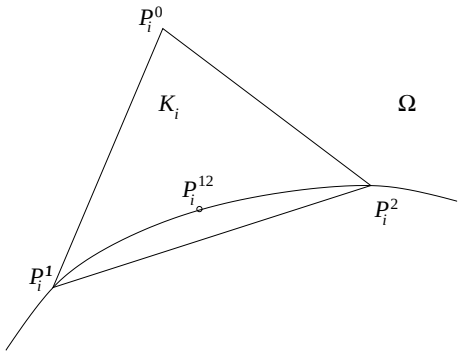

FIG. 3.6. Triangle K_i lying on a curved part of $\partial\Omega$

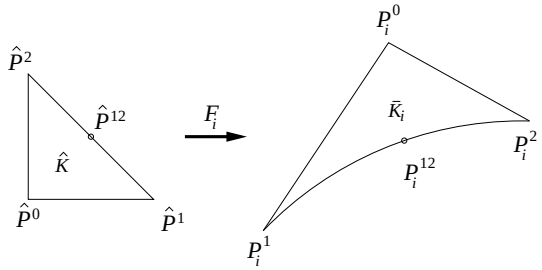

FIG. 3.7. Bilinear mapping $F_i : \hat{K} \to K_i$

found in (Cockburn and Shu, 1998) or (Castillo *et al.*, 2001). However, the use of this approach leads to an extreme increase in the number of unknowns and, therefore, we shall apply another technique, used, for example, in (Oden *et al.*, 1998), (Babuška *et al.*, 1999).

We use the notation from Section 3.2.1.1. Moreover, for $i \in I$, by $\gamma_D(i)$ and $\gamma_N(i)$ we denote the subsets of $\gamma(i)$ formed by such indexes j that the faces Γ_{ij} approximate the parts Γ_D and Γ_N, respectively, of $\partial\Omega$. Thus, we suppose that

$$\gamma(i) = \gamma_D(i) \cup \gamma_N(i), \quad \gamma_D(i) \cap \gamma_N(i) = \emptyset. \tag{3.2.28}$$

For $v \in H^1(\Omega, \mathcal{T}_h)$ we set

$$\begin{aligned} \langle v \rangle_{\Gamma_{ij}} &= \frac{1}{2}\left(v\big|_{\Gamma_{ij}} + v\big|_{\Gamma_{oj}} \right), \\ [v]_{\Gamma_{ij}} &= v\big|_{\Gamma_{ij}} - v\big|_{\Gamma_{ji}}, \end{aligned} \tag{3.2.29}$$

denoting the *average* and *jump of the traces* of v on $\Gamma_{ij} = \Gamma_{ji}$ defined in (3.2.6). The approximate solution as well as test functions are supposed to be elements of the space $S_h = S^{p,-1}(\Omega, \mathcal{T}_h)$ introduced in (3.2.7). Obviously, $\langle v \rangle_{\Gamma_{ij}} = \langle v \rangle_{\Gamma_{ji}}$, $[v]_{\Gamma_{ij}} = -[v]_{\Gamma_{ji}}$ and $[v]_{\Gamma_{ij}} \boldsymbol{n}_{ij} = [v]_{\Gamma_{ji}} \boldsymbol{n}_{ji}$.

In order to derive the discrete problem, we assume that u is a classical solution of problem (3.2.27). The regularity of u implies that $u(\cdot,t) \in H^2(\Omega) \subset H^2(\Omega, \mathcal{T}_h)$ and

$$\begin{aligned} \langle u(\cdot,t) \rangle_{\Gamma_{ij}} = u(\cdot,t)|_{\Gamma_{ij}}, \ [u(\cdot,t)]_{\Gamma_{ij}} = 0, \\ \langle \nabla u(\cdot,t) \rangle_{\Gamma_{ij}} = \nabla u(\cdot,t)|_{\Gamma_{ij}} = \nabla u(\cdot,t)|_{\Gamma_{ji}}, \\ \text{for each } t \in (0,T). \end{aligned} \tag{3.2.30}$$

We multiply equation (3.2.27), a) by any $\varphi \in H^2(\Omega, \mathcal{T}_h)$, integrate over $K_i \in \mathcal{T}_h$, apply Green's theorem and sum over all $K_i \in \mathcal{T}_h$. After some manipulation we obtain the identity

$$\begin{aligned} &\int_\Omega \frac{\partial u}{\partial t}\, \varphi \,\mathrm{d}x + \sum_{i \in I} \sum_{j \in S(i)} \int_{\Gamma_{ij}} \sum_{s=1}^{N} f_s(u)\, (n_{ij})_s\, \varphi|_{\Gamma_{ij}} \,\mathrm{d}S \\ &- \sum_{i \in I} \int_{K_i} \sum_{s=1}^{N} f_s(u)\, \frac{\partial \varphi}{\partial x_s} \,\mathrm{d}x + \sum_{i \in I} \int_{K_i} \nu\, \nabla u \cdot \nabla \varphi \,\mathrm{d}x \\ &- \sum_{i \in I} \sum_{\substack{j \in s(i) \\ j<i}} \int_{\Gamma_{ij}} \nu \langle \nabla u \rangle \cdot \boldsymbol{n}_{ij} [\varphi] \,\mathrm{d}S \\ &- \sum_{i \in I} \sum_{j \in \gamma_D(i)} \int_{\Gamma_{ij}} \nu\, \nabla u \cdot \boldsymbol{n}_{ij}\, \varphi \,\mathrm{d}S \end{aligned} \tag{3.2.31}$$

$$= \int_\Omega g\,\varphi\,\mathrm{d}x + \sum_{i\in I}\sum_{j\in\gamma_N(i)}\int_{\Gamma_{ij}} \nu\,\nabla u\cdot\boldsymbol{n}_{ij}\,\varphi\,\mathrm{d}S.$$

To the left-hand side of (3.2.31) we now add the terms

$$\pm\sum_{i\in I}\sum_{\substack{j\in s(i)\\ j<i}}\int_{\Gamma_{ij}} \nu\langle\nabla\varphi\rangle\cdot\boldsymbol{n}_{ij}[u]\,\mathrm{d}S = 0, \tag{3.2.32}$$

as follows from (3.2.30). Further, to the left-hand side and the right-hand side we add the terms

$$\pm\sum_{i\in I}\sum_{j\in\gamma_D(i)}\int_{\Gamma_{ij}} \nu\,\nabla\varphi\cdot\boldsymbol{n}_{ij}\,u\,\mathrm{d}S$$

and

$$\pm\sum_{i\in I}\sum_{j\in\gamma_D(i)}\int_{\Gamma_{ij}} \nu\,\nabla\varphi\cdot\boldsymbol{n}_{ij}\,u_D\,\mathrm{d}S,$$

respectively, which are identical by the Dirichlet condition (3.2.27), b). We can add these terms equipped with the + sign (the so-called *nonsymmetric DG discretization* of diffusion terms) or with the − sign (*symmetric DG discretization* of diffusion terms). Both possibilities have their advantages and disadvantages – see, for example, (Prudhomme *et al.*, 2000). Here we shall use the nonsymmetric discretization.

In view of the Neumann condition (3.2.27), c), we replace the second term on the right-hand side of (3.2.31) by

$$\sum_{i\in I}\sum_{j\in\gamma_N(i)}\int_{\Gamma_{ij}} g_N\,\varphi\,\mathrm{d}S. \tag{3.2.33}$$

Because of the stabilization of the scheme we introduce the *interior penalty*

$$\sum_{i\in I}\sum_{\substack{j\in s(i)\\ j<i}}\int_{\Gamma_{ij}} \sigma[u]\,[\varphi]\,\mathrm{d}S \tag{3.2.34}$$

and the *boundary penalty*

$$\sum_{i\in I}\sum_{j\in\gamma_D(i)}\int_{\Gamma_{ij}} \sigma\,u\,\varphi\,\mathrm{d}S = \sum_{i\in I}\sum_{j\in\gamma_D(i)}\int_{\Gamma_{ij}} \sigma u_D\varphi\mathrm{d}S \tag{3.2.35}$$

where σ is a *weight* defined by

$$\sigma|_{\Gamma_{ij}} = C_W\nu/\mathrm{d}(\Gamma_{ij}), \tag{3.2.36}$$

where $C_W > 0$ is a suitable constant. In the considered nonsymmetric formulation we can set $C_W = 1$. (For the situation of the symmetric formulation, see Appendix.)

On the basis of the above considerations we introduce the following forms defined for $u,\, \varphi \in H^2(\Omega, \mathcal{T}_h)$:

$$\begin{aligned} a_h(u,\varphi) = &\sum_{i\in I} \int_{K_i} \nu\, \nabla u \cdot \nabla \varphi \,\mathrm{d}x \\ &- \sum_{i\in I} \sum_{\substack{j\in s(i)\\ j<i}} \int_{\Gamma_{ij}} \nu \langle \nabla u \rangle \cdot \boldsymbol{n}_{ij} [\varphi] \,\mathrm{d}S \\ &+ \sum_{i\in I} \sum_{\substack{j\in s(i)\\ j<i}} \int_{\Gamma_{ij}} \nu \langle \nabla \varphi \rangle \cdot \boldsymbol{n}_{ij} [u] \,\mathrm{d}S \\ &- \sum_{i\in I} \sum_{j\in \gamma_D(i)} \int_{\Gamma_{ij}} \nu\, \nabla u \cdot \boldsymbol{n}_{ij}\, \varphi \,\mathrm{d}S \\ &+ \sum_{i\in I} \sum_{j\in \gamma_D(i)} \int_{\Gamma_{ij}} \nu\, \nabla \varphi \cdot \boldsymbol{n}_{ij}\, u \,\mathrm{d}S \end{aligned} \tag{3.2.37}$$

(nonsymmetric variant of the diffusion form - it is obvious what form would have the symmetric variant),

$$\begin{aligned} J_h(u,\varphi) = &\sum_{i\in I} \sum_{\substack{j\in s(i)\\ j<i}} \int_{\Gamma_{ij}} \sigma [u]\, [\varphi] \,\mathrm{d}S \\ &+ \sum_{i\in I} \sum_{j\in \gamma_D(i)} \int_{\Gamma_{ij}} \sigma\, u\, \varphi \,\mathrm{d}S \end{aligned} \tag{3.2.38}$$

(interior and boundary penalty jump terms),

$$\begin{aligned} \ell_h(\varphi)(t) = &\int_\Omega g(t)\, \varphi \,\mathrm{d}x + \sum_{i\in I} \sum_{j\in \gamma_N(i)} \int_\Gamma g_N(t)\, \varphi \,\mathrm{d}S \\ &+ \sum_{i\in I} \sum_{j\in \gamma_D(i)} \int_{\Gamma_{ij}} \nu\, \nabla \varphi \cdot \boldsymbol{n}_{ij}\, u_D(t) \,\mathrm{d}S + \sum_{i\in I} \sum_{j\in \gamma_D(i)} \int_{\Gamma_{ij}} \sigma\, u_D(t)\, \varphi \,\mathrm{d}S \end{aligned} \tag{3.2.39}$$

(right-hand side form).

Finally, the convective terms are approximated with the aid of a numerical flux $H = H(u, v, \boldsymbol{n})$ by the form $b_h(u,\varphi)$ defined analogously as in Section 3.2.1.2:

$$\begin{aligned} b_h(u,\varphi) = &- \sum_{i\in I} \int_K \sum_{s=1}^N f_s(u)\, \frac{\partial \varphi}{\partial x_s} \,\mathrm{d}x \\ &+ \sum_{i\in I} \sum_{j\in S(i)} \int_{\Gamma_{ij}} H\left(u|_{\Gamma_{ij}}, u|_{\Gamma_{ji}}, \boldsymbol{n}_{ij}\right) \varphi|_{\Gamma_{ij}} \,\mathrm{d}S, \quad u,\, \varphi \in H^2(\Omega, \mathcal{T}_h). \end{aligned} \tag{3.2.40}$$

We assume that the numerical flux H is (locally) Lipschitz-continuous, consistent and conservative – see Section 3.2.1.2.

Now we can introduce the *discrete problem.*

Definition 3.5 *We say that u_h is a DGFE solution of the convection-diffusion problem* (3.2.27)*, if*

$$
\begin{aligned}
&a)\ \ u_h \in C^1([0,T]; S_h), \qquad (3.2.41)\\
&b)\ \ \frac{\mathrm{d}}{\mathrm{d}t}(u_h(t),\varphi_h) + b_h(u_h(t),\varphi_h) + a_h(u_h(t),\varphi_h) + J_h(u_h(t),\varphi_h) = \ell_h(\varphi_h)\,(t)\\
&\qquad\quad \forall\,\varphi_h \in S_h,\ \forall\, t \in (0,T),\\
&c)\ \ u_h(0) = u_h^0.
\end{aligned}
$$

By u_h^0 we denote an S_h-approximation of the initial condition u^0.

This discrete problem has been obtained with the aid of the method of lines, i.e. the space semidiscretization. In practical computations suitable time discretization is applied (Euler forward or backward scheme, Runge–Kutta methods or discontinuous Galerkin time discretization) and integrals are evaluated with the aid of numerical integration. Let us note that we do not require here that the approximate solution satisfies the essential Dirichlet boundary condition pointwise, e.g. at boundary nodes. In the DGFEM, this condition is represented in the framework of the 'integral identity' (3.2.41), b).

The above DGFE discrete problem was investigated theoretically in (Dolejší *et al.*, 2002*a*) and (Dolejší *et al.*, 2005), where error estimates were analysed.

3.2.4.3 *DGFE discretization of the Navier–Stokes equations* Similarly as above, one can proceed in the case of the compressible Navier-Stokes equations, but the situation is much more complicated, because the diffusion, i.e. viscous terms, are nonlinear. Therefore, we shall treat the discretization of the viscous terms in a special way, as described in (Dolejší, 2004) or (Feistauer *et al.*, 2005). To this end, we shall linearize partially the viscous terms $\boldsymbol{R}_s(\boldsymbol{w}, \nabla\boldsymbol{w})$ in a suitable way. From (3.1.2) we obtain

$$
\begin{aligned}
&\boldsymbol{R}_1(\boldsymbol{w}, \nabla\boldsymbol{w}) \qquad (3.2.42)\\
&= \begin{pmatrix}
0\\
\frac{2}{3}\,\frac{\mu}{w_1}\left[2\left(\frac{\partial w_2}{\partial x_1} - \frac{w_2}{w_1}\,\frac{\partial w_1}{\partial x_1}\right) - \left(\frac{\partial w_3}{\partial x_2} - \frac{w_3}{w_1}\,\frac{\partial w_1}{\partial x_2}\right)\right]\\
\frac{\mu}{w_1}\left[\left(\frac{\partial w_3}{\partial x_1} - \frac{w_3}{w_1}\,\frac{\partial w_1}{\partial x_1}\right) + \left(\frac{\partial w_2}{\partial x_2} - \frac{w_2}{w_1}\,\frac{\partial w_1}{\partial x_2}\right)\right]\\
\frac{w_2}{w_1}\,\boldsymbol{R}_1^{(2)} + \frac{w_3}{w_1}\,\boldsymbol{R}_1^{(3)} + \frac{k}{c_v w_1}\left[\frac{\partial w_4}{\partial x_1} - \frac{w_4}{w_1}\,\frac{\partial w_1}{\partial x_1}\right.\\
\left. -\frac{1}{w_1}\left(w_2\,\frac{\partial w_2}{\partial x_1} + w_3\,\frac{\partial w_3}{\partial x_1}\right) + \frac{1}{w_1^2}\,(w_2^2 + w_3^2)\,\frac{\partial w_1}{\partial x_1}\right]
\end{pmatrix},
\end{aligned}
$$

$$
\boldsymbol{R}_2(\boldsymbol{w}, \nabla\boldsymbol{w})
$$

$$= \begin{pmatrix} 0 \\ \frac{\mu}{w_1}\left[\left(\frac{\partial w_3}{\partial x_1} - \frac{w_3}{w_1}\frac{\partial w_1}{\partial x_1}\right) + \left(\frac{\partial w_2}{\partial x_2} - \frac{w_2}{w_1}\frac{\partial w_1}{\partial x_2}\right)\right] \\ \frac{2}{3}\frac{\mu}{w_1}\left[2\left(\frac{\partial w_3}{\partial x_2} - \frac{w_3}{w_1}\frac{\partial w_1}{\partial x_2}\right) - \left(\frac{\partial w_2}{\partial x_1} - \frac{w_2}{w_1}\frac{\partial w_1}{\partial x_1}\right)\right] \\ \frac{w_2}{w_1}\boldsymbol{R}_2^{(2)} + \frac{w_3}{w_1}\boldsymbol{R}_2^{(3)} + \frac{k}{c_v w_1}\left[\frac{\partial w_4}{\partial x_1} - \frac{w_4}{w_1}\frac{\partial w_1}{\partial x_2}\right. \\ \left. -\frac{1}{w_1}\left(w_2\frac{\partial w_2}{\partial x_2} + w_3\frac{\partial w_3}{\partial x_2}\right) + \frac{1}{w_1^2}\left(w_2^2 + w_3^2\right)\frac{\partial w_1}{\partial x_2}\right] \end{pmatrix},$$

where $\boldsymbol{R}_s^{(r)} = \boldsymbol{R}_s^{(r)}(\boldsymbol{w}, \nabla\boldsymbol{w})$ denotes the r-th component of $\boldsymbol{R}_s$ ($s = 1, 2,\ r = 2, 3$). Now for $\boldsymbol{w} = (w_1, \ldots, w_4)^{\mathrm{T}}$ and $\boldsymbol{\varphi} = (\varphi_1, \ldots, \varphi_4)^{\mathrm{T}}$ we define the vector-valued functions

$$\boldsymbol{D}_1(\boldsymbol{w}, \nabla\boldsymbol{w}, \boldsymbol{\varphi}, \nabla\boldsymbol{\varphi}) \tag{3.2.43}$$
$$= \begin{pmatrix} 0 \\ \frac{2}{3}\frac{\mu}{w_1}\left[2\left(\frac{\partial \varphi_2}{\partial x_1} - \frac{\varphi_2}{w_1}\frac{\partial w_1}{\partial x_1}\right) - \left(\frac{\partial \varphi_3}{\partial x_2} - \frac{\varphi_3}{w_1}\frac{\partial w_1}{\partial x_2}\right)\right] \\ \frac{\mu}{w_1}\left[\left(\frac{\partial \varphi_3}{\partial x_1} - \frac{\varphi_3}{w_1}\frac{\partial w_1}{\partial x_1}\right) + \left(\frac{\partial \varphi_2}{\partial x_2} - \frac{\varphi_2}{w_1}\frac{\partial w_1}{\partial x_2}\right)\right] \\ \frac{w_2}{w_1}\boldsymbol{D}_1^{(2)} + \frac{w_3}{w_1}\boldsymbol{D}_1^{(3)} + \frac{k}{c_v w_1}\left[\frac{\partial \varphi_4}{\partial x_1} - \frac{\varphi_4}{w_1}\frac{\partial w_1}{\partial x_1}\right. \\ \left. -\frac{1}{w_1}\left(w_2\frac{\partial \varphi_2}{\partial x_1} + w_3\frac{\partial \varphi_3}{\partial x_1}\right)\right. \\ \left. +\frac{1}{w_1^2}\left(w_2\varphi_2 + w_3\varphi_3\right)\frac{\partial w_1}{\partial x_1}\right] \end{pmatrix},$$

$$\boldsymbol{D}_2(\boldsymbol{w}, \nabla\boldsymbol{w}, \boldsymbol{\varphi}, \nabla\boldsymbol{\varphi})$$
$$= \begin{pmatrix} 0 \\ \frac{\mu}{w_1}\left[\left(\frac{\partial \varphi_3}{\partial x_1} - \frac{\varphi_3}{w_1}\frac{\partial w_1}{\partial x_1}\right) + \left(\frac{\partial \varphi_2}{\partial x_2} - \frac{\varphi_2}{w_1}\frac{\partial w_1}{\partial x_2}\right)\right] \\ \frac{2}{3}\frac{\mu}{w_1}\left[2\left(\frac{\partial \varphi_3}{\partial x_2} - \frac{\varphi_2}{w_1}\frac{\partial w_1}{\partial x_2}\right) - \left(\frac{\partial \varphi_2}{\partial x_1} - \frac{\varphi_2}{w_1}\frac{\partial w_1}{\partial x_1}\right)\right] \\ \frac{w_2}{w_1}\boldsymbol{D}_2^{(2)} + \frac{w_3}{w_1}\boldsymbol{D}_2^{(3)} + \frac{k}{c_v w_1}\left[\frac{\partial \varphi_4}{\partial x_2} - \frac{\varphi_4}{w_1}\frac{\partial w_1}{\partial x_2}\right. \\ \left. -\frac{1}{w_1}\left(w_2\frac{\partial \varphi_2}{\partial x_2} + w_2\frac{\partial \varphi_3}{\partial x_2}\right)\right. \\ \left. +\frac{1}{w_1^2}\left(w_2\varphi_2 + w_3\varphi_3\right)\frac{\partial w_1}{\partial x_2}\right] \end{pmatrix},$$

where $\boldsymbol{D}_s^{(r)}$ denotes the r-th component of $\boldsymbol{D}_s$ ($s = 1, 2,\ r = 2, 3$). Obviously, $\boldsymbol{D}_1$ and $\boldsymbol{D}_2$ are linear with respect to $\boldsymbol{\varphi}$ and $\nabla\boldsymbol{\varphi}$ and

$$\boldsymbol{D}_s(\boldsymbol{w}, \nabla\boldsymbol{w}, \boldsymbol{w}, \nabla\boldsymbol{w}) = \boldsymbol{R}_s(\boldsymbol{w}, \nabla\boldsymbol{w}), \quad s = 1, 2. \tag{3.2.44}$$

Now we introduce the following forms defined for functions $\boldsymbol{w}_h, \boldsymbol{\varphi}_h \in \mathcal{S}_h$:

$$(\boldsymbol{w}_h, \boldsymbol{\varphi}_h)_h = \int_{\Omega_h} \boldsymbol{w}_h \cdot \boldsymbol{\varphi}_h \,\mathrm{d}x \tag{3.2.45}$$

($L^2(\Omega_h)$-scalar product),

$$\begin{aligned} a_h(\boldsymbol{w}_h, \boldsymbol{\varphi}_h) = & \sum_{i\in I} \int_{K_i} \sum_{s=1}^{2} \boldsymbol{R}_s(\boldsymbol{w}_h, \nabla \boldsymbol{w}_h) \cdot \frac{\partial \boldsymbol{\varphi}_h}{\partial x_s} \,\mathrm{d}x \\ & - \sum_{i\in I} \sum_{\substack{j\in s(i)\\ j<i}} \int_{\Gamma_{ij}} \sum_{s=1}^{2} \langle \boldsymbol{R}_s(\boldsymbol{w}_h, \nabla \boldsymbol{w}_h)\rangle \, (n_{ij})_s \cdot [\boldsymbol{\varphi}_h] \,\mathrm{d}S \\ & + \sum_{i\in I} \sum_{\substack{j\in s(i)\\ j<i}} \\ & \int_{\Gamma_{ij}} \sum_{s=1}^{2} \langle \boldsymbol{D}_s(\boldsymbol{w}_h, \nabla \boldsymbol{w}_h, \boldsymbol{\varphi}_h, \nabla \boldsymbol{\varphi}_h)\rangle \, (n_{ij})_s \cdot [\boldsymbol{w}_h] \,\mathrm{d}S \\ & - \sum_{i\in I} \sum_{j\in \gamma_D(i)} \int_{\Gamma_{ij}} \sum_{s=1}^{2} \boldsymbol{R}_s(\boldsymbol{w}_h, \nabla \boldsymbol{w}_h) \, (n_{ij})_s \cdot \boldsymbol{\varphi}_h \,\mathrm{d}S \\ & + \sum_{i\in I} \sum_{j\in \gamma_D(i)} \\ & \int_{\Gamma_{ij}} \sum_{s=1}^{2} \boldsymbol{D}_s(\boldsymbol{w}_h, \nabla \boldsymbol{w}_h, \boldsymbol{\varphi}_h, \nabla \boldsymbol{\varphi}_h) \, (n_{ij})_s \cdot \boldsymbol{w}_h \,\mathrm{d}S \end{aligned} \tag{3.2.46}$$

(nonsymmetric version of the diffusion form). The use of the above special approach does not yield some additional terms in the discrete analogy to the continuity equation. This appears important for a good quality of the approximate solution.

Further, we introduce the following forms:

$$\begin{aligned} J_h(\boldsymbol{w}_h, \boldsymbol{\varphi}_h) = & \sum_{i\in I} \sum_{\substack{j\in s(i)\\ j<i}} \int_{\Gamma_{ij}} \sigma [\boldsymbol{w}_h] \cdot [\boldsymbol{\varphi}_h] \,\mathrm{d}S \\ & + \sum_{i\in I} \sum_{j\in \gamma_D(i)} \int_{\Gamma_{ij}} \sigma \, \boldsymbol{w}_h \cdot \boldsymbol{\varphi}_h \,\mathrm{d}S \end{aligned} \tag{3.2.47}$$

with

$$\sigma|_{\Gamma_{ij}} = \mu / d(\Gamma_{ij}) \tag{3.2.48}$$

(interior and boundary penalty terms),

$$\beta_h(\boldsymbol{w}_h, \boldsymbol{\varphi}_h) = \sum_{i\in I} \sum_{j\in \gamma_D(i)} \int_{\Gamma_{ij}} \Big(\sigma \, \boldsymbol{w}_B \cdot \boldsymbol{\varphi}_h \tag{3.2.49}$$

$$+\sum_{s=1}^{2} \boldsymbol{D}_s(\boldsymbol{w}_h, \nabla \boldsymbol{w}_h, \boldsymbol{\varphi}_h, \nabla \boldsymbol{\varphi}_h)\,(n_{ij})_s \cdot \boldsymbol{w}_B \Big)\,\mathrm{d}S$$

(right-hand side form). The boundary state $\boldsymbol{w}_B$ will be defined later. Finally, we define the form approximating viscous terms:

$$\begin{aligned} &A_h(\boldsymbol{w}_h, \boldsymbol{\varphi}_h) \\ &\quad = a_h(\boldsymbol{w}_h, \boldsymbol{\varphi}_h) + J_h(\boldsymbol{w}_h, \boldsymbol{\varphi}_h) - \beta_h(\boldsymbol{w}_h, \boldsymbol{\varphi}_h). \end{aligned} \tag{3.2.50}$$

The convective terms are represented by the form b_h defined by (3.2.16).

Now the *discrete problem* reads: Find a vector-valued function $\boldsymbol{w}_h$ such that

$$\begin{aligned} &\text{a)}\ \ \boldsymbol{w}_h \in C^1([0,T]; \boldsymbol{S}_h), \\ &\text{b)}\ \ \frac{\mathrm{d}}{\mathrm{d}t}\left(\boldsymbol{w}_h(t), \boldsymbol{\varphi}_h\right)_h + b_h\left(\boldsymbol{w}_h(t), \boldsymbol{\varphi}_h\right) + A_h\left(\boldsymbol{w}_h(t), \boldsymbol{\varphi}_h\right) \\ &\qquad\qquad = 0 \quad \forall\, \boldsymbol{\varphi}_h \in \boldsymbol{S}_h,\ t \in (0,T), \\ &\text{c)}\ \ \boldsymbol{w}_h(0) = \boldsymbol{w}_h^0, \end{aligned} \tag{3.2.51}$$

where $\boldsymbol{w}_h^0$ is an $\boldsymbol{S}_h$-approximation of $\boldsymbol{w}^0$.

3.2.4.4 *Boundary conditions* If $\Gamma_{ij} \subset \partial\Omega_h$, i.e. $j \in \gamma(i)$, it is necessary to specify boundary conditions.

The boundary state $\boldsymbol{w}_B = (w_{B1}, \ldots, w_{B4})^{\mathrm{T}}$ is determined with the aid of the prescribed Dirichlet conditions and extrapolation:

$$\begin{aligned} &\boldsymbol{w}_B = (\rho_{ij}, 0, 0, \rho_{ij}\theta_{ij}) \quad \text{on } \Gamma_{ij} \text{ approximating } \Gamma_W, \\ &\boldsymbol{w}_B = \left(\rho_{Dh}, \rho_{Dh}v_{Dh1}, \rho_{Dh}v_{Dh2}, \rho_{Dh}\theta_{Dh} + \frac{1}{2}\rho_{Dh}|\boldsymbol{v}_{Dh}|^2\right) \\ &\qquad \text{on } \Gamma_{ij} \text{ approximating } \Gamma_I, \end{aligned} \tag{3.2.52}$$

where ρ_{Dh}, θ_{Dh} and $\boldsymbol{v}_{Dh} = (v_{Dh1}, v_{Dh2})$ are approximations of the given density, absolute temperature and velocity from the boundary conditions and ρ_{ij}, θ_{ij} are the values of the density and absolute temperature extrapolated from K_i onto Γ_{ij}.

The boundary state $\boldsymbol{w}|_{\Gamma_{ji}}$ appearing in the form b_h is defined in the same way as in Section 3.2.1.3 above.

3.2.5 *Numerical examples*

In the DGFE solution of problems presented here, the forward Euler time discretization was used.

3.2.5.1 *Application of the DGFEM to the solution of inviscid compressible flow* The first numerical example deals with inviscid transonic flow through the GAMM channel with inlet Mach number = 0.67. In order to obtain a steady-state solution, the time stabilization method for $t \to \infty$ is applied.

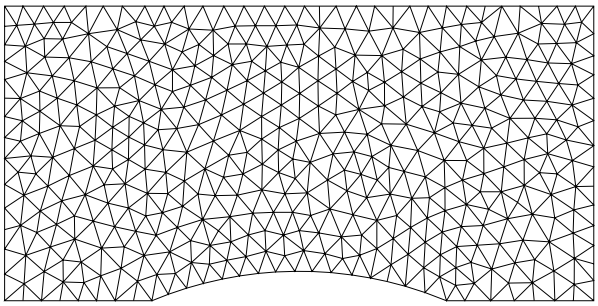

FIG. 3.8. Coarse triangular mesh (784 triangles) in the GAMM channel

We demonstrate the influence of the use of superparametric elements at the curved part of $\partial\Omega$, explained in Section 3.2.3. The computations were performed on a coarse grid shown in Fig. 3.8 having 784 triangles. Figures 3.9 and 3.10 show the density distribution along the lower wall obtained by scheme (3.2.21) without and with the use of a bilinear mapping, respectively. One can see a difference in the quality of the approximate solutions.

Figure 3.11 shows the computational grid constructed with the aid of the anisotropic mesh adaptation (AMA) technique ((Dolejší, 1998), (Dolejší, 2001)). Figure 3.12 shows the density distribution along the lower wall obtained with the aid of the bilinear mapping on a refined mesh. As we can see, a very sharp shock wave and the so-called Zierep (small local maximum behind the shock wave) singularity were obtained.

3.2.5.2 *Application of the DGFEM to the solution of viscous compressible flow* We present here results of the numerical solution of the viscous supersonic flow past the airfoil NACA 0012 by the DGFEM with far field Mach number $M_\infty = 2$ and Reynolds number $Re = 1000$. In Fig. 3.13 we see the mesh obtained by the with the aid of the anisotropic mesh adaptation (AMA) technique. Fig. 3.14 shows the Mach number isolines. Here we see a shock wave in front of the profile, wake and a shock wave leaving the profile.

In the above examples, the forward Euler time stepping and limiting of the order of accuracy from Section 3.2.2 were used. This method requires to satisfy the CFL stability condition representing a severe restriction of the time step. In (Dolejší and Feistauer, 2003), an efficient semi-implicit time stepping scheme was developed for the numerical solution of the Euler equations, allowing to use a long time step in the DGFEM. This method even allows the solution of flows with very low Mach numbers. The extension to viscous flow is in progress.

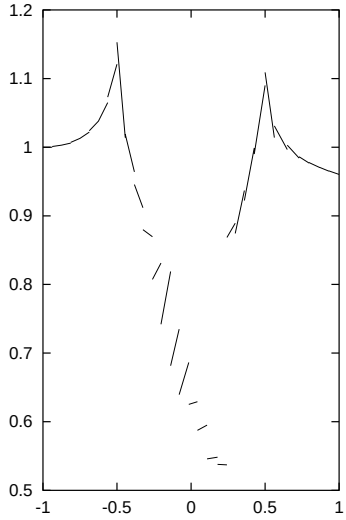

FIG. 3.9. Density distribution along the lower wall in the GAMM channel without the use of a bilinear mapping at $\partial\Omega$

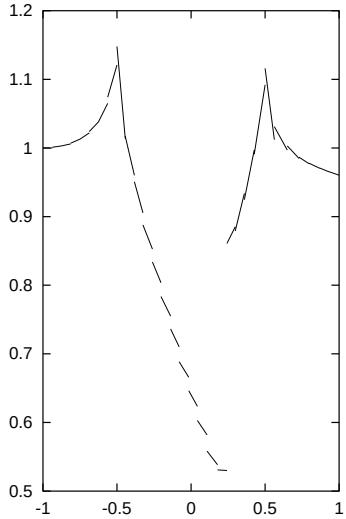

FIG. 3.10. Density distribution along the lower wall in the GAMM channel with the use of a bilinear mapping at $\partial\Omega$

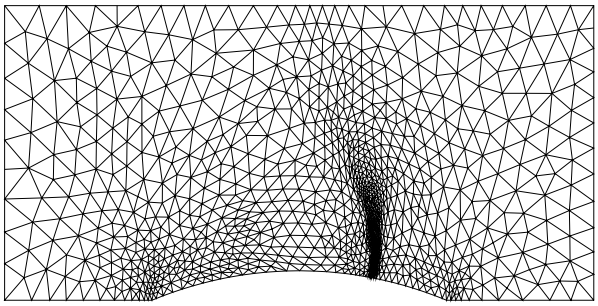

FIG. 3.11. Adapted triangular mesh (2131 triangles) in the GAMM channel

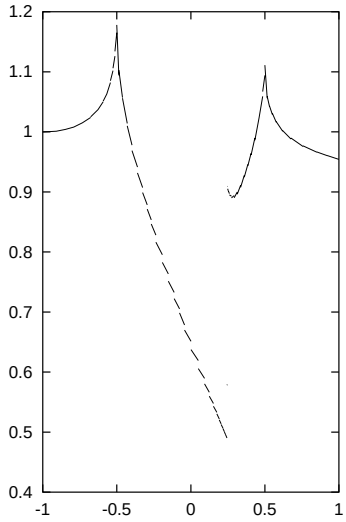

FIG. 3.12. Density distribution along the lower wall in the GAMM channel with the use of a bilinear mapping on an adapted mesh

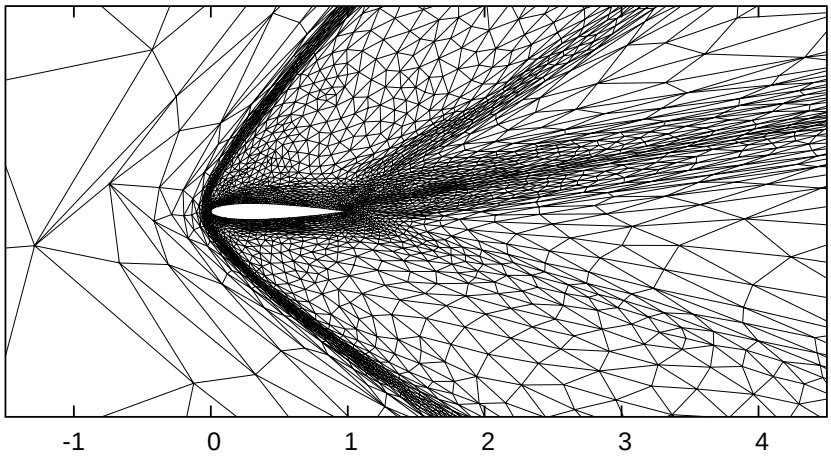

FIG. 3.13. Viscous supersonic flow past the profile NACA 0012: triangulation

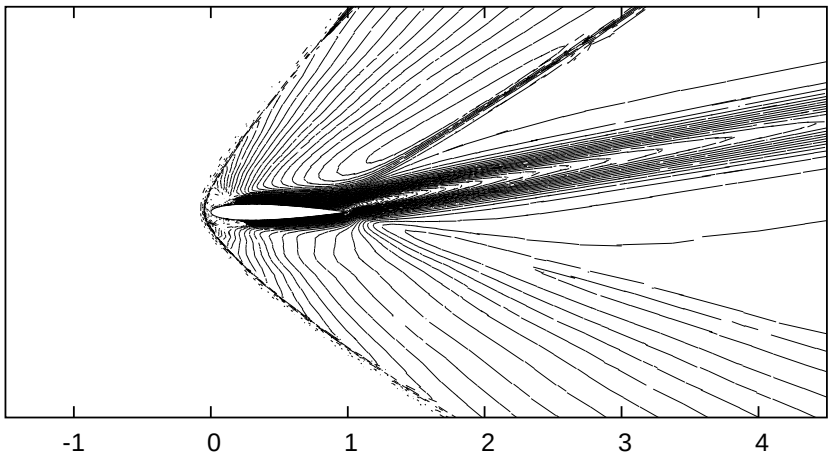

FIG. 3.14. Viscous supersonic flow past the profile NACA 0012: Mach number isolines

REFERENCES

Angot, Ph., Dolejší, V., Feistauer, M., and Felcman, J. (1998). Analysis of a combined barycentric finite volume – nonconforming finite element method for nonlinear convection–diffusion problems. *Appl. Math.*, **43(4)**, 263–310.

Babuška, I., Oden, J. T., and Baumann, C. E. (1999). A discontinuous *hp* finite element method for diffusion problems: 1-D analysis. *Comput. Math. Appl.*, **37**, 103–122.

Bassi, F. and Rebay, S. (1997*a*). A high-order accurate discontinuous finite element method for the numerical solution of the compressible Navier–Stokes equations. *J. Comput. Phys*, **131**, 267–279.

Bassi, F. and Rebay, S. (1997*b*). High-order accurate discontinuous finite element solution of the 2D Euler equations. *J. Comput. Phys.*, **138**, 251–285.

Castillo, P., Cockburn, B., Schötzau, D., and Schwab, C. (2001). Optimal a priori error estimates for the *hp*-version of the local discontinuous Galerkin method for convection–diffusion problems. *Math. Comput.*, **71**, 455–478.

Ciarlet, P. G. (1979). *The Finite Element Method for Elliptic Problems*. North-Holland, Amsterdam.

Cockburn, B. (1999). Discontinuous Galerkin methods for convection dominated problems. In *High-Order Methods for Computational Physics* (ed. T. J. Barth and H. Deconinck), Number 9 in Lecture Notes in Computational Science and Engineering, pp. 69–224. Springer, Berlin.

Cockburn, B. and Shu, C. W. (1998). The local discontinuous Galerkin finite element method for convection–diffusion systems. *SIAM J. Numer. Anal.*, **35**, 2440–2463.

Crouzeix, M. and Raviart, P. A. (1973). Conforming and nonconforming finite element methods for solving the stationary Stokes equations. *RAIRO, Anal. Numér.*, **7**, 33–76.

Dolejší, V. (1998). Anisotropic mesh adaptation for finite volume and finite element methods on triangular meshes. *Comput. Visualization Sci.*, **1(3)**, 165–178.

Dolejší, V. (2001). Anisotropic mesh adaptation technique for viscous flow simulation. *East–West J. Numer. Math.*, **9(1)**, 1–24.

Dolejší, V. (2004). On the discontinuous Galerkin method for the numerical solution of the Euler and Navier–Stokes equations. *Int. J. Numer. Meth. Fluids*.

Dolejší, V. and Feistauer, M. (2003). A semiimplicit discontinuous Galerkin finite element method for the numerical solution of inviscid compressible flows. The Preprint Series of the School of Mathematics MATH-KNM-2003/2, Charles University, Prague.

Dolejší, V., Feistauer, M., Felcman, J., and Kliková, A. (2002). Error estimates

for barycentric finite volumes combined with nonconforming finite elements applied to nonlinear convection–diffusion problems. *Appl. Math.*, **47(4)**, 301–340.

Dolejší, V., Feistauer, M., and Schwab, C. (2002*a*). A finite volume discontinuous Galerkin scheme for nonlinear convection–diffusion problems. *Calcolo*, **39**, 1–40.

Dolejší, V., Feistauer, M., and Schwab, C. (2002*b*). On discontinuous Galerkin methods for nonlinear convection–diffusion problems and compressible flow. *Math. Bohemica*, **127(2)**, 163–179.

Dolejší, V., Feistauer, M., and Schwab, C. (2003). On some aspects of the discontinuous Galerkin finite element method for conservation laws. *Math. Comput. Simul.*, **61**, 333–346.

Dolejší, V., Feistauer, M., and Sobotíková, V. (2005). Analysis of the discontinuous Galerkin method for nonlinear convection–diffusion problems. *Comput. Methods. Appl. Mech. Engrg.*, **194**, 2709–2733.

Eymard, R., Gallouët, T., and Herbin, R. (2000). *Handbook of Numerical Analysis*, Volume VII, Chapter Finite Volume Methods, pp. 717–1020. North-Holland-Elsevier, Amsterdam.

Feistauer, M. (1993). *Mathematical Methods in Fluid Dynamics*. Longman Scientific & Technical, Harlow.

Feistauer, M. (2002). Discontinuous Galerkin method: Compromise between FV and FE schemes. In *Finite Volumes for Complex Applications III* (ed. R. Herbin and D. Kröner), pp. 81–96. Hermes Penton Science, London.

Feistauer, M., Dolejší, V., and Kučera, V. (2005). On the discontinuous Galerkin method for the simulation of compressible flow with wide range of Mach numbers. The Preprint Series of the School of Mathematics MATH-KNM-2005/5, Charles University, Prague.

Feistauer, M. and Felcman, J. (1997). Theory and applications of numerical schemes for nonlinear convection–diffusion problems and compressible viscous flow. In *The Mathematics of Finite Elements and Applications, Highlights 1996* (ed. J. Whiteman), pp. 175–194. Wiley, Chichester.

Feistauer, M., Felcman, J., and Dolejší, V. (1996). Numerical simulation of compresssible viscous flow through cascades of profiles. *ZAMM*, **76**, 297–300.

Feistauer, M., Felcman, J., and Lukáčová-Medviďová, M. (1995). Combined finite element–finite volume solution of compressible flow. *J. Comput. Appl. Math.*, **63**, 179–199.

Feistauer, M., Felcman, J., and Lukáčová-Medviďová, M. (1997). On the convergence of a combined finite volume–finite element method for nonlinear convection–diffusion problems. *Numer. Methods Partial Differ. Equations*, **13**, 163–190.

Feistauer, M., Felcman, J., Lukáčová-Medviďová, M., and Warnecke, G. (1999*a*). Error estimates of a combined finite volume–finite element method for nonlinear convection–diffusion problems. *SIAM J. Numer. Anal.*, **36(5)**, 1528–1548.

Feistauer, M., Slavík, J., and Stupka, P. (1999*b*). On the convergence of a combined finite volume–finite element method for nonlinear convection–diffusion problems. Explicit schemes. *Numer. Methods Partial Differ. Equations*, **15**, 215–235.

Karniadakis, G. E. and Sherwin, S. J. (1999). *Spectral/hp Element Methods for CFD*. Oxford University Press, Oxford.

Oden, J. T., Babuška, I., and Baumann, C. E. (1998). A discontinuous *hp* finite element method for diffusion problems. *J. Comput. Phys*, **146**, 491–519.

Prudhomme, S., Pascal, F., Oden, J. T., and Romkes, A. (2000). Review of a priori error estimation for discontinuous Galerkin methods. Technical report, TICAM.

INDEX